



## Review Article

# Non-human Primate Models of Alzheimer's Disease



Yihan Li<sup>1</sup> and Ben J. Gu<sup>1,2\*</sup>

<sup>1</sup>The Florey Institute, The University of Melbourne, Parkville, Australia; <sup>2</sup>National Clinical Research Centre for Aging and Medicine, Huashan Hospital, Fudan University, Shanghai, China

Received: January 29, 2023 | Revised: March 02, 2023 | Accepted: March 10, 2023 | Published online: April 20, 2023

### Abstract

Alzheimer's disease (AD) is a chronic neurodegenerative disorder characterised by cognitive impairment and numerous pathologies, including  $\beta$ -amyloid ( $A\beta$ ) and Tau proteopathies, altered immune responses, and brain atrophy. Despite hundreds of years of investigations into its underlying pathogenesis, the aetiology of AD is not clearly understood. AD diagnostic criteria are not effective at identifying pre-clinical patients and current AD treatments cannot postpone or reverse disease progression. The development of non-human primate (NHP) models of AD is urgently required due to their close phylogenetic relationship to humans, similar neuroanatomy, comparable genetics, and high complexity of high-order cognitive functions, making them a better model of AD than rodents. We compared and contrasted AD-associated pathological features and behavioural alterations manifested between naturally aged spontaneous and induced NHP models of AD. Induced models of AD can be established using injections of  $A\beta$  oligomers, brain homogenates, neurotoxins, or formaldehyde. In recent decades, both spontaneous and induced NHP models of AD have been used to facilitate the development of neuroimaging tracers and therapeutic treatments, aiding in the translational application of lab discoveries into clinical trials involving human subjects. The establishment of a standardised NHP model of AD is expected by making a guideline concerning NHP species, types and doses of inducers, frequency of injections, and duration of inoculation. Its development can be facilitated by a comprehensive assessment of NHPs, including all AD-associated pathologies and a wide range of behavioural examinations. NHP models of AD have contributed to AD research and their evolution is expected to better recapitulate AD features and present greater translational potential in the near future.

**Keywords:** Rhesus monkey; Cynomolgus monkey; Tree shrews; Squirrel monkeys; Mouse lemurs.

**Abbreviations:** 3R Tau, Tau isoforms with 3 repeats; 4R Tau, Tau isoforms with 4 repeats; AChE, acetylcholinesterase enzyme; AD, Alzheimer's disease; ApoE, apolipoprotein E; ApoJ, apolipoprotein J; APP, amyloid precursor protein;  $A\beta$ , beta-amyloid;  $A\beta$ 1-40,  $A\beta$  ending in residue 40;  $A\beta$ 1-42,  $A\beta$  ending in residue 42;  $A\beta$ ,  $A\beta$  oligomer; BDNF, brain-derived neurotrophic factor; CAA, cerebral amyloid angiopathy; CSF, cerebrospinal fluid; DMT, disease-modifying treatments; DMTS, delayed match to sample; DNMS, delayed nonmatching-to-sample; DR, delayed response; DRST, delayed recognition span task; EEG, electroencephalogram; EOAD, early-onset AD; FA, formaldehyde; GFAP, glial fibrillary acidic protein; GSM,  $\gamma$ -secretase modulators; ICV- $A\beta$ , intracerebroventricular administration of  $A\beta$ ; ICV-STZ, intracerebroventricular injection of STZ; IT- $A\beta$ , intrathecal administration of  $A\beta$ ; LOAD, late-onset AD; M4, the fourth subtype of mAChR; mAb, monoclonal antibodies; mAChR, M1 muscarinic acetylcholine receptor; MAPT, microtubule-associated protein Tau; NFT, neurofibrillary tangles; NHP, non-human primate; NMDA, N-methyl-D aspartate; NT, neuropil threads; PET, positron emission tomography; PHF, paired helical filaments; PSEN1, presenilin 1; PSEN2, presenilin 2; P-Tau, hyperphosphorylated Tau; P-Tau181P, Tau phosphorylated at threonine 181; P-Tau231P, Tau phosphorylated at threonine 231; SNP, single nucleotide polymorphisms; STM, short-term memory; STZ, streptozotocin; t-Tau, total Tau.

\*Correspondence to: Ben J. Gu, The Florey Institute, The University of Melbourne, 30 Royal Parade, Parkville, Victoria 3052, Australia. ORCID: <https://orcid.org/0000-0001-5500-4453>. Tel: +61 3 9035 6317, Fax: +61 3 9035 3100, E-mail: [ben.gu@florey.edu.au](mailto:ben.gu@florey.edu.au)

**How to cite this article:** Li Y, Gu BJ. Non-human Primate Models of Alzheimer's Disease. *J Explor Res Pharmacol* 2023;8(3):199–221. doi: 10.14218/JERP.2023.00006.

### Introduction of Alzheimer's disease (AD)

#### Background of AD

AD is a devastating neurodegenerative disorder that constitutes 70–80% of all dementia cases worldwide.<sup>1</sup> It is clinically manifested by deterioration in learning, episodic memory, visuospatial orientation, and executive abilities that eventually deprive patients' capabilities of performing daily activities.<sup>1,2</sup> Pathologically, AD is characterised by brain atrophy at the macroscopic level, and extracellular senile plaques, intracellular neurofibrillary tangles (NFT), and glial cell engagement at the microscopic level.<sup>3</sup> Macroscopically, the brains of AD patients are marked by moderate cortical atrophy and enlarged sulcal spaces in the frontal and temporal cortices, which characterise the final stage of dementia in disease progress, but is not specific to AD.<sup>3</sup> Currently, scientists define the pre-clinical phase of AD as the cellular phase, during which alterations of proteopathies, neurons, and glial cells drive disease progression before the clinical presentation of cognitive impairment and executive deficits.<sup>4,5</sup> Correspondingly, the diagnostic criteria of AD have shifted from the gold-standard post-mortem examination of parenchymal beta-amyloid ( $A\beta$ ) and Tau proteopathies to the current suite of biofluid biomarkers and molecular imaging.<sup>6</sup>

A $\beta$  neuroimaging by positron emission tomography (PET) and cerebrospinal fluid (CSF) measurements of A $\beta$ , total Tau (t-Tau), and hyperphosphorylated Tau (p-Tau) allow an accurate diagnosis of individuals with pre-clinical and prodromal AD.<sup>5</sup> However, the costliness and invasiveness of molecular neuroimaging and CSF measurements limit their application as a population-based screening technique in hospital settings.<sup>6</sup> Since the first identification and classification of AD in the last century, and despite decades of extensive efforts, cost-effective early diagnostic tools, effective disease-modifying treatments (DMT), and a sophisticated understanding of AD pathogenesis, much about AD remains inconclusive.<sup>2</sup> With the ongoing aging of the global population, this devastating chronic disease will impose extensive economical, psychological, and physical burdens on individuals, families, and countries.

### *A $\beta$ -related pathologies*

As first described over 100 years ago, the classical pathological features of AD include extracellular A $\beta$  plaques and intracellular NFTs.<sup>1</sup> A $\beta$  plaques are the aggregated form of A $\beta$  peptides, including A $\beta$  peptides ending in residue 40 (A $\beta$ <sub>1-40</sub>) and ending in residue 42 (A $\beta$ <sub>1-42</sub>), both of which result from the abnormal processing of amyloid precursor protein (APP) by  $\beta$ - and  $\gamma$ -secretases.<sup>3,7</sup>  $\beta$ -secretase cleaves the juxta-membrane domain of APP and generates the ectodomain, after which  $\gamma$ -secretase cleaves multiple sites in the transmembrane domain of APP, leading to the production of carboxy terminal fragments and A $\beta$  peptides, ranging from 38 to 43 residues.<sup>3,7</sup> Among these 4.5kDa A $\beta$  peptides, A $\beta$ <sub>1-42</sub> is the most hydrophobic, fibrillogenic, and amyloidogenic component, which corresponds with its high neurotoxicity in AD.<sup>7</sup> Two types of A $\beta$  plaques have been mainly observed in AD, namely diffuse plaques, and dense core plaques. Diffuse plaques are weakly stained by thioflavin-S and are deprived of activated glial cells or neuritic components, while dense core plaques can be intensely stained by thioflavin-S and Congo red due to the presence of numerous A $\beta$  fibrils.<sup>3</sup> Dense core plaques are usually associated with Tau<sup>+</sup> or dystrophic neurites, which are also known as neuritic plaques.<sup>3</sup> In the peripheral zone of dense core neuritic plaques, some dystrophic neurites contain Tau filaments, suggesting the presence of NFT-bearing neurons in that region.<sup>3</sup> Other types of dystrophic neurites may contain cytoskeletal proteins or may become accumulated by degenerating mitochondria and lysosomal bodies.<sup>3</sup> Considering the complicated molecular and cellular components of A $\beta$  plaques, investigating the mechanism underlying plaque formation, A $\beta$  neurotoxicity, immune activation, neuronal loss, and Tau involvement is critical to advance our understanding of AD pathogenesis and cognitive decline. Beyond the composition of A $\beta$  plaques, A $\beta$  peptides aggregate and propagate in stereotypic patterns in AD, leading to the staging schemes described by Braak and Thal.<sup>8</sup> Thal has improved the three-stage Braak staging into an advanced five-stage scheme: A $\beta$  deposits in neocortex exclusively in phase one; A $\beta$  spreads into the allocortical brain regions in phase two; A $\beta$  further spreads into diencephalic nuclei, the striatum, and the cholinergic nuclei of the basal forebrain in phase three; A $\beta$  further spreads into several brainstem nuclei in phase four; A $\beta$  eventually propagates into the cerebellum in phase five.<sup>8</sup> In human AD, the abnormal production of A $\beta$  and the imbalanced clearance of A $\beta$  results in the aberrant deposition of A $\beta$  plaques in the brains of AD patients, during which Tau pathologies, neuronal swelling, cytoskeletal abnormalities, intracellular organelle dysfunction, and glial activation are engaged. This is extremely challenging to replicate in animal models of AD.

In addition to the brain parenchyma, A $\beta$  peptides are also deposited in the walls of small- to medium-sized blood vessels of the brain, which is known as cerebral amyloid angiopathy (CAA). The walls of leptomeningeal and cortical arteries and occasionally, veins, are predominantly occupied by A $\beta$ <sub>1-40</sub> peptides, while A $\beta$ <sub>1-42</sub> peptides are the main component of neuritic plaques in the parenchyma.<sup>9</sup> Parenchymal A $\beta$  plaques and CAA can both be caused by A $\beta$  peptides with a common origin, suggesting a potential shared mechanism driving both A $\beta$  proteopathies.<sup>9</sup> A $\beta$ <sub>1-42</sub> peptides may first be deposited in the vessel wall, while A $\beta$ <sub>1-40</sub> peptides may subsequently be deposited in the walls along the perivascular drainage pathways, while fibrillogenic neuron-derived A $\beta$ <sub>1-42</sub> peptides are more likely to deposit in the parenchyma to form A $\beta$  plaques.<sup>9</sup> Parenchymal A $\beta$  plaques originate in the neocortex of the brain and subsequently propagate into the allocortex, thalamus, and basal ganglia, but CAA may predominantly affect the posterior lobar brain regions and rarely deposit in the deep grey nuclei, white matter, and brainstem.<sup>9</sup> Additionally, A $\beta$  peptides in the walls of vessels are amalgamated with A $\beta$ -associated proteins, including complement proteins, apolipoprotein E (ApoE), and apolipoprotein J (ApoJ/CLU). As the two major A $\beta$  proteopathies in AD pathophysiology, CAA and parenchymal A $\beta$  plaques may share a common origin of A $\beta$  peptides, metabolism, and clearance mechanisms, while different lengths of A $\beta$  peptides, different A $\beta$ -associated proteins, and different associations with cognitive deficits are noted.






### *Tau-related pathologies*

A solid neuropathological diagnosis of human AD requires the detection of both A $\beta$  plaques and NFTs, the latter of which is more tightly associated with synaptic loss and cognitive impairment.<sup>10</sup> Tau filaments are termed as paired helical filaments (PHF) because they comprise two filaments that twist to form a periodic structure.<sup>3</sup> In AD, PHFs are structured by six isoforms of Tau, including isoforms with 3 repeats (3R Tau) and 4-repeats (4R Tau) in the microtubule binding domain. These isoforms are generated through alternative splicing of the microtubule-associated protein Tau (MAPT) gene (chr17).<sup>3,11</sup> Axonal Tau plays an important role by interacting with tubulin, stabilising microtubule structure, and supporting microtubule-dependent axonal transport.<sup>11</sup> Pathophysiologically, Tau can be hyperphosphorylated with nine phosphates per molecule, resulting in fibrillation of p-Tau and aggregation into NFTs.<sup>11</sup> These molecular alterations undermine its original abilities to bind and stabilise microtubules in axons, thus resulting in the deposition of intraneuronal lesions, including p-Tau, pre-tangle materials, NFTs in cell bodies, neuropil threads (NT) in neuronal processes, and other materials in neuritic plaques.<sup>12</sup> In the brains of AD patients, the distribution pattern and sequence of Tau lesions have also been categorised in three stages, as described by Braak and colleagues.<sup>12</sup> Abnormal Tau is initially detected in transentorhinal and entorhinal regions, gradually spreading to the limbic allocortex and adjoining neocortex, and eventually propagating to the primary and secondary fields.<sup>12</sup>

### *AD genetics*

AD can be divided into early-onset AD (EOAD) and late-onset AD (LOAD) based on the age of onset. EOAD accounts for less than 1% of total AD cases. It is determined by autosomal dominant mutations in genes encoding APP (*APP*), presenilin 1 (*PSEN1*) and presenilin 2 (*PSEN2*). Mutations in the *APP* gene generally predispose APP to be cleaved by  $\beta$ -secretase, leading to the production of more A $\beta$ <sub>1-42</sub> peptides that aggregate and propagate easily.<sup>13</sup>

**Table 1.** The most widely used NHP in the field of AD

Animal species	Rhesus macaques	Cynomolgus monkeys	Squirrel monkeys	Mouse lemurs	Tree shrews
Classification	Old world monkey	Old world monkey	New world monkey	Prosimian	Non primate
Scheme					
General background					
Scientific name	<i>Macaca mulattas</i>	<i>Macaca fascicularis</i>	<i>Simia sciurea</i>	<i>Microcebus murinus</i>	<i>Tupaia belangeri chinensis</i>
Body length	45–64 cm	40–65 cm	25–35 cm	12–13 cm	26–41 cm
Weight	5–12 kg	9 kg	0.5–1.1 kg	50–120 g	50–270 g
Life span	34–40 years	35 years	15–20 years	8–14 years	8 years
Age considered old	20–25 years old	20 years old	12 years old	5 years old	7 years old
	Recruited in references				

NHP, non-human primate; AD, Alzheimer's disease.

Mutations in *PSEN1* and *PSEN2* change the specificity of cleavage sites on APP, preferring to be cleaved at position 42 instead of 40, also resulting in more  $A\beta_{1-42}$  production.<sup>14</sup> Numerous mutations in EOAD genes converge on the same outcome of altered proteolytic APP processing and  $A\beta_{1-42}$  overproduction, which forms the foundation of the  $A\beta$ -amyloid theory.<sup>7</sup> LOAD accounts for the remaining 99% of total AD cases, and is currently explained by the imbalanced production and clearance of  $A\beta$  in the brain.<sup>1</sup> The risk of an individual developing LOAD is largely determined by common polymorphisms in the *APOE* gene. This gene encodes the glycoprotein ApoE that is ubiquitously expressed in the brain, liver, and myeloid cells, and which plays a role in cholesterol and lipid transportation, neuronal growth, and immunoregulation.<sup>15</sup> The *APOE* gene encodes three isoforms: protective ApoE  $\epsilon 2$ , neutral ApoE  $\epsilon 3$ , and detrimental ApoE  $\epsilon 4$ .<sup>15</sup> Two different amino acids in the three isoforms significantly modify the structure and function of ApoE, resulting in alterations in  $A\beta$  clearance, lipid metabolism, glucose metabolism, innate immune responses, and mitochondrial dysfunction.<sup>16</sup> For instance, CAA in capillaries, arterioles, and small arteries are highly associated with ApoE  $\epsilon 4$ , which might be explained by the reduced transendothelial clearance of  $A\beta$ -apolipoprotein complexes compared with ApoE  $\epsilon 2$  and ApoE  $\epsilon 3$  carriers.<sup>3</sup> The precise mechanism by which *APOE*  $\epsilon 4$  increases AD risk remains inconclusive, thus further investigation of the *APOE* gene in AD is critical for advancing our understanding of AD.

### Animal models of AD

Despite extensive investigations into AD for over 100 years, the underlying pathophysiological mechanisms remain unknown, the disease aetiology is still insufficiently understood, accurate diagnostic tools cannot be widely applied for population screening, and the DMTs are lacking. In light of these urgent demands in the field, the development and study of reliable animal models of AD becomes essential to enable the study of the pre-clinical and prodromal phase

of AD, which is difficult to access in AD patients.<sup>2</sup> A wide range of species have been assessed in AD-related research and various rodent models of AD have dominated the field in recent decades.<sup>2</sup> Genetic mutations associated with  $A\beta$  and Tau processing have provided a solid foundation for generating hundreds of transgenic murine models that have evolved over time to imitate specific features of AD and facilitate the translational application of laboratory discoveries.<sup>17</sup> Rodent models have many advantages, including low financial costs, large sample sizes, easier genetic manipulation, conventional animal care, etc. Unfortunately, rodents are also associated with low translational potential for the development of diagnostic markers and therapeutic treatments due to the reduced complexity of their brain structure and circuitry compared to humans.<sup>2</sup> For instance, APP transgenic mice rarely manifest the Tau hyperphosphorylation and brain atrophy that are found in human AD.<sup>2</sup> Thus, to understand a complicated age-related human disorder, using the brain of a non-human primate (NHP) with a closer phylogenetic relationship to humans, a similar neuroanatomy structure, comparable genetics, similarly complicated neural circuitry, and higher-order cognitive functions is greatly preferred (Table 1).

### Normal aging studies in NHPs

Aging is the single largest risk factor for AD.<sup>1</sup> Although aged NHPs cannot recapitulate the full spectrum of AD, they are ideal models of normal aging, cognitive deterioration, and executive processing impairment. Since the 1970s, numerous studies have reported age-related impairments in cognition in a wide range of animals, particularly NHPs, including short-term memory (STM), learning abilities, and executive functions, which have been similarly documented during aging of human.<sup>18</sup> The Rhesus monkey (*Macaca mulattas*), an old world monkey closely relative to the cynomolgus monkeys, has been predominantly employed in early studies that investigated the association between learning impairment, memory dysfunction, and normal aging in NHPs.<sup>19</sup> Rhesus monkeys have a body length of

45–64 cm, a body weight of 5–12 kg, and a life expectancy of 34–40 years (Table 1).<sup>20</sup> In 1978, Bartus and colleagues used an indirect delayed response (DR) procedure and identified a profound impairment in STM in the aged ( $\geq 18$  years old) compared to younger (3–5 years old) rhesus monkeys.<sup>21</sup> STM is defined as the ability of an individual to temporarily memorise a limited amount of information for a very short interval. Deficits in STM are one of the best characterised alterations in normal aging.<sup>18,22</sup> STM deterioration in rhesus monkeys emerged in early middle age during normal aging, similar to what is observed in humans.<sup>18</sup> They further evaluated monkeys' abilities to learn visual discrimination and reversal problems.<sup>23</sup> The aged rhesus monkeys ( $\geq 18$  years old) constantly demonstrated severe deficiency with reversal problems, but no age-related deterioration in colour and pattern discrimination was observed.<sup>23</sup> Another concept that is closely associated with STM is working memory that temporarily stores, processes, and manipulates STM necessary for complicated cognitive tasks, such as language comprehension, learning, and reasoning.<sup>22</sup> A decline in the working memory of aged primates has been documented in several NHP studies using a neurotoxin-induced model of AD.<sup>24–27</sup>

The seminal studies conducted by Bartus and colleagues failed to identify age-related impairment in recognition memory, but they inspired subsequent studies in this field. In 1987, rhesus monkeys of four different age groups were trained in a delayed nonmatching-to-sample (DNMS) task that examined the subject's ability to recognise a novel object from a familiar object, following a specific delay interval.<sup>18,28</sup> Although their learning abilities were marginally impaired with aging, significant age-related impairment in recognising objects were observed when delay intervals or lists of objects were increased.<sup>28</sup> This study contradicted Bartus' previous results and identified impairment in visual recognition memory during normal aging of NHPs.<sup>28</sup> The DNMS task was also used later on female aged rhesus monkeys (22–26 years old).<sup>29</sup> The aged rhesus monkeys required significantly more training than young monkeys (9–11 years old) to learn basic principles of the task, but their recognition memory was minimally impaired compared with the young, consistent with Bartus' results.<sup>29</sup> Rapp and colleagues then required rhesus monkeys to remember the order of subjects and identified significant age-related deterioration in their task-dependent recognition memory.<sup>29</sup> These findings further suggested different susceptibilities to age-related impairment in different memory functions in NHPs. In 1993, Bachevalier conducted a more comprehensive investigation into memory functions of rhesus monkeys by selecting multiple memory tasks associated with distinct brain areas.<sup>30</sup> This study described widespread behavioural deficits in aged rhesus monkeys, including visuospatial orientation, DR tasks, and object recognition memory (measured using DNMS) in young middle/teen age, middle age, and old age of rhesus monkey, respectively.<sup>30</sup> These memory abilities are associated with different brain regions, illustrating that certain cerebral systems were predisposed to early degenerative neuronal damage.<sup>30</sup> Delayed recognition span tasks (DRST) are another important recognition memory task, in which NHPs are required to recognise a novel stimuli among an increasing array of serially presented stimuli to examine their spatial and colour condition.<sup>31</sup> It was used to assess the recognition memory of eight aged rhesus monkeys (25–27 years old) that presented with recognition memory impairment in both the spatial and colour conditions of the DRST.<sup>31</sup> Visuospatial orientation was also compromised in young middle/teen age in rhesus monkeys compared with other memory deficits.<sup>30</sup> The impairment in recognition memory is not associated with the age-related decline in the length of cholinergic fibres of rhesus

monkeys.<sup>32</sup> Some controversies were observed in these studies, but age-associated abnormalities in recognition memory among aged NHPs are supported by increasing evidence as technology has improved, and sample sizes have increased. During normal aging, NHPs manifest similar symptoms to human AD, particularly cognitive behavioural alterations, suggesting their potential to be used as a model of age-related neurodegenerative disorders.

## Spontaneous NHP models of AD

### *A $\beta$* pathologies in aged NHPs

Aged NHPs demonstrate cognitive deficits that are similarly observed in aged humans, but also spontaneously develop age-associated human AD-resembling pathologies, such as extracellular A $\beta$  plaques, CAA, intracellular p-Tau, dystrophic neurites, and glial activation. All aged NHP species exhibit A $\beta$ -related proteopathies in their cerebellum and vasculature, but differences in the age of onset, burden level, biological composition, and spatial distribution are still observed.<sup>2</sup> In 1985, numerous A $\beta$  plaques in the prefrontal and temporal cortices in six aged rhesus monkeys were identified, the densities of which were significantly associated with age, suggesting a positive association between age and A $\beta$  burden in aged NHPs.<sup>33</sup> Subsequent studies identified similar results in the frontal, temporal, and parietal cortices of aged rhesus monkeys and aged squirrel monkeys, as measured by thioflavin-S and silver staining.<sup>34–36</sup> The total burden level of parenchymal A $\beta$  in the temporal and occipital cortices of aged rhesus monkeys was comparable to those of humans with AD, while the A $\beta_{1-40}$  level may outweigh the A $\beta_{1-42}$  level in aged rhesus monkeys.<sup>37</sup> The highest A $\beta$  plaque densities were noticed in the frontal and temporal cortices, while few A $\beta$  peptides were deposited in the hippocampal formation, highly resembling the A $\beta$  distribution in human AD.<sup>37,38</sup> Another type of old-world monkeys that have been extensively used in this field is the cynomolgus monkey (*Macaca fascicularis*), also known as crab-eating macaques (Table 1).<sup>20</sup> Cynomolgus monkeys have a body length of 40–65 cm, a body weight of up to 9 kg, and a life expectancy of up to 35 years (Table 1).<sup>20</sup> Both diffuse and classical A $\beta$  plaques with dense cores were detected primarily in the temporal cortex of the superior and inferior gyri and amygdala in aged cynomolgus monkeys.<sup>39,40</sup> These A $\beta$  plaques were surrounded by abnormal, swollen neurites in silver-stained sections,<sup>34–36,40</sup> similar to what is reported in human AD.<sup>2</sup> Aged old-world monkeys illustrated similar A $\beta$  plaques in the parenchyma compared to the brains of humans diagnosed with AD. More examinations into the pathologies and behavioural alterations are required to designate them as suitable animal models of AD.

Squirrel monkeys (*Simia sciurea*), a widely used new-world monkey, have a body length of 25–35 cm, a body weight of 0.5–1.1 kg, and life expectancy of 15–20 years (Table 1). The smaller body and shorter life expectancy of aged squirrel monkeys explain the deposition of smaller A $\beta$  plaques in their cerebellum at a relatively younger age ( $\sim 12$  years old) compared with rhesus monkeys ( $\sim 25$  years old).<sup>19,35</sup> Like rhesus monkeys, A $\beta_{1-40}$  is the more abundant peptide in the brains of aged squirrel monkeys, in contrast to human AD.<sup>41,42</sup> C-terminal specific antibodies against A $\beta_{1-40}$  and A $\beta_{1-42}$  were used to evaluate the A $\beta$  burden in the brains of 11 rhesus monkeys (21–31 years) and one 59-year-old chimpanzee.<sup>41</sup> In rhesus monkeys, A $\beta_{1-40}^+$  plaques outnumbered A $\beta_{1-42}^+$  plaques with a mean ratio of 2.08, which was significantly higher than the ratio of A $\beta_{1-40}^+$ :A $\beta_{1-42}^+$  plaques in human AD (0.37).<sup>41</sup> Similar results were observed in another study using two aged Formosan

rock macaques (*Macaca cyclopis*), which are close relatives to rhesus monkeys.<sup>42</sup> The high A $\beta_{1-40}$  burden level in aged NHPs may be caused by different APP processing mechanisms or altered A $\beta$ -ApoE interaction, which favours the production of A $\beta_{1-40}$  in aged NHPs.<sup>42</sup> These early studies recognised the age-associated A $\beta$  burden level and widespread distribution in the brains of aged NHPs, which highly resembled human AD despite the distinct levels of A $\beta_{1-40}$  and A $\beta_{1-42}$ . A wide range of recent studies have all repeated the identification of this classical human AD-resembling A $\beta$  proteopathy in the brains of various NHPs, utilizing more advanced experimental techniques to elucidate the interaction between A $\beta$  plaques, AD genetics, glial activation, and Tau hyperphosphorylation in these spontaneous NHP model of AD.<sup>40,43-52</sup>

The tree shrew is also a small primate used as a NHP model of AD, in particular the Chinese tree shrew (*Tupaia belangeri chinensis*) (Table 1). They have body lengths of 26–41 cm, body weights of 50–270 g, and a life expectancy of 8 years old (Table 1). In one early study, Pawlik and colleagues did not identify A $\beta$  deposits in the neural parenchyma or cerebral vasculature of eight aged tree shrews (7–8 years old).<sup>53</sup> Subsequent studies using anti-A $\beta_{1-42}$  antibodies detected A $\beta$  depositions in the cortex, subiculum, basal ganglia, mammillary body, and hypothalamus, accompanied by weak Congo red<sup>+</sup> A $\beta$  plaques in the brains of aged tree shrews.<sup>54</sup>

Another A $\beta$ -related pathology, CAA, may be more consistent than parenchymal A $\beta$  deposits in aged NHPs.<sup>2</sup> Thioflavin-S<sup>+</sup> A $\beta$  plaques in the walls of intracortical and meningeal microvessels of aged rhesus monkeys and aged squirrel monkeys were identified.<sup>34-36</sup> Uno and colleagues conducted a well-powered study using the brains of 81 rhesus monkeys (16–39 years old).<sup>45</sup> Young rhesus monkeys (16–19 years old) did not manifest parenchymal A $\beta$  plaques, while the majority of the aged monkeys (26–39 years old) presented numerous A $\beta$  depositions in their brains.<sup>45</sup> CAA developed simultaneously with parenchymal A $\beta$  plaques after the age of 20 years old, and was detected in 38% of the oldest rhesus monkeys, suggesting a lower frequency of CAA compared with parenchymal A $\beta$  plaques in aged rhesus monkeys.<sup>45</sup> CAA was also observed in other species of aged old-world monkeys.<sup>39,40</sup> In contrast to the relatively low vascular A $\beta$  deposits in aged old-world monkeys, cerebrovascular A $\beta$  is the most abundant form of A $\beta$  proteopathy in squirrel monkeys.<sup>55,56</sup> Three forms of A $\beta$  deposits were identified in nine squirrel monkeys (8–27 years old) from high to low density: dense A $\beta$  deposits to the vascular wall, classical parenchymal A $\beta$  plaques with a dense core, and diffuse A $\beta$  plaques.<sup>55</sup> Among the four aged squirrel monkeys, the ratio of CAA to dense parenchymal A $\beta$  plaques was over 5.<sup>55</sup> Although A $\beta_{1-42}$  and A $\beta_{1-40}$  were detected in both parenchymal and cerebrovascular plaques, more A $\beta_{1-40}$  existed in CAA in the larger arterioles of aged squirrel monkeys.<sup>56</sup> One remarkable difference between humans and squirrel monkeys is the heavy deposition of A $\beta$  in the capillaries, suggesting species-specific predispositions of vulnerable cerebral vasculature to A $\beta$  pathology.

In addition to old and new world monkeys, mouse lemurs (*Microcebus murinus*), a prosimian resembling the earliest primates, have been frequently used to study normal aging of NHPs (Table 1).<sup>2</sup> Mouse lemurs are characterised by a small body length of 12 cm and a tail with a similar length (Table 1).<sup>20,46</sup> They have a small body weight of 50–120 g and a short life expectancy of 8–14 years (Table 1).<sup>20,46</sup> Bons and colleagues first utilised mouse lemurs to study A $\beta$  proteopathies during normal aging of NHPs.<sup>44</sup> They compared eight aged mouse lemurs (8–12 years old) with three young mouse lemurs (1–3 years old), and recognised three forms of A $\beta$  proteopathies in the brains, including round thiofla-

vin-S<sup>+</sup> A $\beta$  plaques, round A $\beta$  plaques with a thioflavin-S<sup>+</sup> dense core, and extensive A $\beta$  deposits in leptomeningeal, cortical arteries and arterioles, and occasionally, capillaries.<sup>44</sup> Only half of the aged mouse lemurs exhibited parenchymal A $\beta$  plaques, whose size resembled those observed in rhesus monkeys and humans. All aged mouse lemurs demonstrated extensive CAA, suggesting a higher frequency of CAA compared with that of human AD.<sup>44</sup> Mestre-Frances and colleagues further investigated the A $\beta$  compositions of CAA in aged NHPs using 30 mouse lemurs (2–13 years old).<sup>57</sup> Intensive deposits of A $\beta_{1-42}$  were observed in the cortical arteriole and capillary walls, but A $\beta_{1-40}$  deposits were mainly noticed in the tunica media of leptomeningeal vessels, where A $\beta_{1-42}$  was weakly detected.<sup>57</sup> This study illustrated a promising NHP model of AD concerning the similarities in A $\beta$  proteopathies compared to human AD, including high parenchymal burden of A $\beta_{1-42}$  and high vascular deposition of A $\beta_{1-40}$ . Cognitive impairment of the aged mouse lemur is another essential criterion to be assessed. Schmidtke and colleagues recruited 37 aged mouse lemurs (>5 years old) and identified significant associations between cortical A $\beta$  burden level and pretraining success (intraneuronal A $\beta$ ) and discrimination learning (extracellular A $\beta$ ).<sup>51</sup> Even though the accumulation of A $\beta$  in the walls of neocortical vessels were detected, no association between CAA and cognitive decline was found.<sup>51</sup> A $\beta$  proteopathies in the aged mouse lemur were also documented in recent studies, in which the interactions between A $\beta$ , Tau, genetic factors, and immune cells were further elaborated.<sup>43,58</sup>

#### A $\beta$ -associated genetics and proteins in aged NHPs

AD is a complicated disorder determined by both genetic and environmental factors. Both EOAD and LOAD are largely influenced by genetic mutations or single nucleotide polymorphisms (SNP) that result in the overproduction of amyloidogenic A $\beta_{1-42}$  and impaired clearance of A $\beta$  peptides. The differences in A $\beta$  proteopathies between aged NHPs and humans with AD inspire another question regarding whether A $\beta$ -associated genetics and proteins are different between humans and NHPs. Full-length cDNA encoding APP<sub>695</sub> of aged cynomolgus monkeys were sequenced, demonstrating 100% sequence homology to human, while two amino acid substitutions were reported in APP<sub>695</sub> of rats and mice.<sup>39</sup> None of the EOAD-associated mutations were found in the lemur APP gene.<sup>46</sup> The common longer isoforms in aged cynomolgus monkeys, APP<sub>751</sub> and APP<sub>770</sub>, demonstrated a few amino acid substitutions compared with human APP.<sup>39</sup> The brain homogenates of humans and monkeys demonstrated a similar profile of membrane-associated, full-length APP, and truncated isoforms of APP, in contrast to the profile of rat and mouse brains, suggesting highly similar proteolytic processing of APP between NHPs and human.<sup>39</sup> APP was also detected in the swollen neurites of classical A $\beta$  plaques but absent in diffuse A $\beta$  plaques in the brain of aged cynomolgus monkeys.<sup>40</sup> In aged rhesus monkeys, APP was detected in swelling neurons and neuritic plaques associated with A $\beta$ .<sup>59</sup> In mouse lemurs, an APP sequence analysis of exon 16 and 17, which encodes for A $\beta$ , illustrated 100% homology with human A $\beta$ , suggesting conserved RNA splicing in mouse lemurs and humans.<sup>58</sup> A $\beta$  and APP were simultaneously detected in A $\beta$  plaques and CAA, while APP itself was further deposited in neurons, astrocytes, and oligodendrocytes.<sup>58</sup> The labelling level of APP was significantly associated with age in mouse lemurs, suggesting a more sophisticated distribution of APP and A $\beta$  proteopathies in aged mouse lemurs.<sup>58</sup> Additionally, the activity of  $\beta$ -secretase (BACE1) was increased with age in both rhesus monkeys and humans, while its expression level remained the same.<sup>60</sup> The genetic

background of the tree shrew has also been investigated and their primary sequences of APP revealed 98% similarity and 97% identity to human APP.<sup>53</sup> A high-quality reference genome of Chinese tree shrews has been recently generated and their expression pattern of A $\beta$  and NFT formation pathway genes resembled that of human brain, with a similar aging-dependent effect.<sup>61,62</sup> Both genetic sequences and distributive patterns of APP and A $\beta$  are highly conserved between multiple species of NHPs and human, making them ideal models of AD with higher genetic homology.

EOAD-associated PSEN1 and PSEN2 have also been investigated in NHPs. The cDNA encoding PSEN1 from mouse lemurs exhibited 95.3% sequence similarity with human PSEN1, which was slightly higher than murine PSEN1.<sup>63</sup> The 2% difference between lemur and mouse PSEN1 showed the conservation of a particular proteolytic processing in both lemur and human.<sup>63</sup> PSEN1 was detected in neurons and neurites in multiple cortical layers, hippocampus, and subcortical structures in aged mouse lemurs.<sup>63</sup> Another study specifically cloned a 1340 bp cDNA fragment encoding PSEN2 from a mouse lemur brain that demonstrated 95.5% homology to human PSEN2 and 93.5% homology to mouse PSEN2.<sup>64</sup> None of the EOAD-associated PSEN1 or PSEN2 mutations in humans corresponded to lemur PSEN1 and PSEN2 amino acid differences.<sup>46</sup> PSEN2 was distributed throughout the lemur brain, including dense signals in the cortical and subcortical structures and cerebral vessels, and light signals in the hippocampal neurons and the dentate gyrus.<sup>64</sup> The co-localisation of PSEN1, PSEN2, and APP was observed, but only age-related increase in *PSEN2* expression was noticed in the lemur brain.<sup>63,64</sup> Lemur APP, PSEN1, and PSEN2 showed higher homology to human proteins than those of rats and mice, suggesting a higher degree of conservation between lemurs and humans. Furthermore, the age-related expressions of *PSEN1* and *PSEN2* were also investigated in the brain of cynomolgus monkeys. PSEN1 was detected in neurons and neuritic plaques in the neocortex and cerebellum of cynomolgus monkeys and PSEN1 levels in the nuclear fraction were significantly elevated with age, indicating age-related PSEN1 accumulation in the endoplasmic reticulum associated with the nuclear membrane.<sup>65</sup> On the contrary, PSEN2 was also detected in large pyramidal neurons and neuritic plaques, but its expression level remained unchanged during aging of cynomolgus monkeys.<sup>66</sup> Recently, PSEN2 mRNA in the Chinese tree shrew has been characterised, demonstrating 97.64% sequence similarity to human PSEN2.<sup>67</sup> Even though the protein structure of PSEN2 indicates similarities to human PSEN2, tree shrew PSEN2 possesses only seven  $\alpha$ -helices, while human PSEN2 contains ten  $\alpha$ -helices.<sup>67</sup> These observations suggest a more important involvement of PSEN1 compared with PSEN2 in disease progression of NHPs, but more studies are needed to elucidate their roles and functions in NHP compared with those of humans.

Beyond EOAD-associated genetics, APOE remains the single largest genetic risk factor for AD in humans. In mouse lemurs, APOE genotyping revealed monomorphisms that possessed the two diagnostic sites that defined the ApoE  $\epsilon$ 4 allele of human, albeit with 9 amino acid substitutions compared with human ApoE.<sup>68</sup> One type of vervet monkey, the *Caribbean vervet*, was also found to be homozygous for the ApoE  $\epsilon$ 4 allele.<sup>69</sup> APOE was heavily deposited in line with A $\beta$  proteopathies, including the parenchymal A $\beta$  plaques and CAA.<sup>68</sup> APOE was further detected in astrocytes of the cortical parenchyma, oligodendrocytes of the corpus callosum, and neurons of multiple cortical lobes, the hippocampus, and the brainstem of the aged mouse lemur.<sup>68</sup> Like mouse lemurs and humans, APOE was detected in diffuse and classical A $\beta$  plaques

and meningeal and cortical vessels in the brains of aged chimpanzees, cynomolgus monkeys, and rhesus monkeys, while old-world monkeys exhibited more neuritic plaques with APOE staining.<sup>40,70</sup> In cynomolgus monkeys, APOE was detected in some astrocytes and mononuclear cells around cortical blood vessels, co-localising with glial fibrillary acidic protein (GFAP) in astrocytes.<sup>40</sup> Additionally, APOE genetics were also studied in aged vervet monkeys (*Chlorocebus aethiops*), illustrating ApoE  $\epsilon$ 4 monomorphism among 30 vervet monkeys.<sup>69</sup> In brief, NHPs are homozygous for ApoE  $\epsilon$ 4 that is highly detrimental in human AD. This interesting discrepancy between NHPs and humans makes it necessary to understand the protective mechanism underlying why these ApoE  $\epsilon$ 4 homozygotes display dense parenchymal and vascular A $\beta$  plaques, but never develop the devastating cognitive decline and behavioural alterations observed in humans diagnosed with AD.

### *Tau pathologies in aged NHPs*

Unlike human AD, NFTs are virtually lacking in the brains of aged NHPs.<sup>2</sup> Only a few old-world monkeys, new-world monkeys, and prosimians illustrated NFTs and dystrophic neurites near neuritic plaques in early studies.<sup>2</sup> In aged rhesus monkeys (30–31 years old) with cerebral A $\beta$  plaques, PHF<sup>+</sup> or Tau<sup>+</sup> NFTs or A $\beta$  plaques were absent in their brains using antiserum while this same antiserum generated intensive signals in the brains of human with AD.<sup>34</sup> In a recent study, the monoclonal antibody (mAb), AT8, against a phosphorylated epitope of human Tau protein detected sparsely scattered p-Tau in the cingulate cortex in the brains of aged old-world monkeys, including Campbell's guenon and Hamadryas baboon.<sup>71</sup> AT8<sup>+</sup> p-Tau was detected in the entorhinal cortex and hippocampus of one 28-year-old rhesus monkey, which was simultaneously confirmed using AT100, PHF-1, and TG-3 antibodies, illustrating a similar distribution pattern to Tauopathy in the brains of human with AD.<sup>71</sup> Meanwhile, another five 28-year-old rhesus monkeys exhibited high A $\beta$  burdens in their prefrontal cortices but no Tau AT8 immunoreactivity, suggesting rare p-Tau immunoreactivity in aged rhesus monkeys around 30 years.<sup>71</sup> Even though rhesus monkeys exhibit human AD-resembling A $\beta$  depositions and glial activation, the low incidence of Tauopathy during their normal aging may restrict their suitability as a NHP model of AD. In 2018, a cohort of rhesus monkeys from young to extreme old age ( $\leq$ 38 years old) illustrated similar qualitative patterns and sequences of Tau and A $\beta$ , highly resembling human AD.<sup>49</sup> P-Tau was initially detected in cell islands, dendritic microtubules, and transporting endosomes of the entorhinal cortex in young rhesus monkeys (7–9 years old) (like Braak stage I).<sup>49</sup> In early aged rhesus monkeys (24–26 years old), AT8 immunoreactivity was mildly detected in the outer layer II of the entorhinal cortex with one case illustrating cognitive impairment (like Braak stage I/II).<sup>49</sup> In aged rhesus monkeys (33–34 years old), AT8 labelling further propagated intensively and widely throughout cell islands of the layer II and occasionally in the deeper entorhinal cortex (like Braak stage III).<sup>49</sup> Surprisingly, mature NFTs were recognised in both layer II and V of the entorhinal cortex in the oldest rhesus monkey (38 years old) (like Braak III/IV).<sup>49</sup> Given the co-existence of parenchymal A $\beta$  plaques, CAA, and intracellular A $\beta$  in endosomes, dendrites, and exons, this study first demonstrated human AD-resembling Tauopathies, especially NFTs, in extremely aged NHPs, although the low incidence was distinct from that of human AD.<sup>49</sup> Subsequently, a cohort of nine female rhesus monkeys (8.3–28.6 years old) demonstrated pyramidal cells labelled with AT8 and pT217 antibodies in the dorsolateral prefrontal cortex, which are currently used in CSF diagnosis of human AD.<sup>72</sup> These pT217<sup>+</sup>

pyramidal cells contained aggregated, filamentous structures that highly resembled NFTs in human AD.<sup>72</sup> While early studies hardly ever detected Tau signals in aged rhesus monkeys, recent studies have demonstrated that rhesus monkeys can naturally develop p-Tau, filamentous structures, and rare NFTs, suggesting a promising NHP model of AD that assist in elucidating the associations between A $\beta$ , p-Tau, and cognitive deficits in AD.

PHF- and Tau-specific antibodies did not detect any NFTs or neuritic plaques in the brains of aged cynomolgus monkeys (19 years old) and aged chimpanzees (59 years old) in early studies.<sup>39,40,70</sup> Of note, very limited numbers of neurons in the lateral putamen region of three aged chimpanzees were slightly labelled with Alz-50 (against p-Tau).<sup>70</sup> In 2010, a cohort of 24 cynomolgus monkeys (6–36 years old) were found to have A $\beta$  plaques in their neocortical and hippocampal regions in middle age, which was associated with age rather than p-Tau accumulation.<sup>47</sup> Intracellular p-Tau was first detected in neurons and oligodendrocytes in the temporal cortex and hippocampus of cynomolgus monkeys in a 19-year-old cynomolgus monkey using 2B11 (against human Tau phosphorylated at amino acid 231).<sup>47</sup> In humans over 20 years of age, 2B11<sup>+</sup> glial cells increased proportionally with age, but 2B11<sup>+</sup> neurons were only detected in a 36-year-old cynomolgus monkey, in which a strong p-Tau signal was occasionally detected in neurons, oligodendrocytes, and dystrophic neurites in its temporal cortex.<sup>47</sup> Interestingly, the number of 2B11<sup>+</sup> neurons in this 30-year-old monkey was smaller than that of the 19-year-old monkey, which might be explained by a specific conformational change of Tau under pathological conditions by an unknown mechanism.<sup>47</sup> Later, another 21 brains of cynomolgus monkeys (7–36 years old) were studied for A $\beta$  and Tau proteopathies.<sup>52</sup> A $\beta$  plaques were detected in eight brains of monkeys at 24 years old, while p-Tau deposits were found in only five brains from monkeys over 30 years old, suggesting a similar sequence of AD-associated lesions to humans with AD.<sup>52</sup> AT8<sup>+</sup> p-Tau lesions were distributed predominantly in oligodendrocyte-like cells throughout the white matter and basal ganglia, which was different from p-Tau patterns in human with AD, mainly in the hippocampus.<sup>52</sup> Only 4R Tau was detected with AT8 immunoreactivity, which was diffuse and granular in the neuronal cytoplasm and dendrites, instead of NFT organisations.<sup>52</sup> In old-world monkeys, the co-existence of A $\beta$  and Tau proteopathies were detected in normal aging, during which human AD-resembling A $\beta$  plaques and CAA were deposited earlier, while human AD-resembling NFTs were rarely detected. The classical amyloid theory states that neurotoxic A $\beta$  peptides induce subsequent Tau phosphorylation, NFT accumulation, glial activation, and neuronal death, as demonstrated by close associations between A $\beta$  and p-Tau lesions in the brains of human with AD. Therefore, at least in old-world monkeys, the accumulation of p-Tau and, occasionally NFTs, merely reflected the age-dependent hyperphosphorylation and aggregation of Tau induced by A $\beta$ .<sup>47</sup>

Tau and p-Tau in mouse lemurs have been well investigated in many studies while NFTs are rarely observed.<sup>68,73</sup> In early studies, Tau deposits in mouse lemurs were morphologically and biochemically different from NFTs observed in humans with AD, similarly to those in old-world monkeys.<sup>74</sup> A well-powered quantitative analysis of Tau recruited 40 mouse lemurs (1–13 years old).<sup>74</sup> By using 961-S28T, Tau accumulations (maybe PHF) were found in the frontal cortex, the occipital cortex, and the parietal and temporal cortices, the prevalence, and densities of which were associated with age in both young and old groups.<sup>74</sup> Quantitatively, aged mouse lemurs ( $\geq 8$  years old) exhibited significantly higher Tau burdens than the young in all neocortical areas, subiculum, and

amygdala, while the entorhinal cortex, subiculum, and amygdala were affected by Tau in the aged group exclusively.<sup>74</sup> In contrast to Tau distribution in mouse lemurs, the frontal cortex usually exhibited low NFT burden, while hippocampal formation was predisposed to Tauopathy in the brains of human with AD.<sup>12</sup> These contradictions suggest a different neuronal vulnerability to Tauopathy in the neocortex of mouse lemurs and humans.<sup>74</sup> More specifically, Tau proteins were modified and aggregated in granules close to the membrane of the neuronal perikaryal and dendrites in the aged mouse lemur.<sup>46</sup> Aggregated p-Tau reactive to PHF antibodies were detected with A $\beta$  and ApoE in neurons and oligodendrocytes in the neocortex and hippocampus, as well as vascular A $\beta$  depositions.<sup>46,68</sup> Co-localisation of p-Tau and PSEN2 was occasionally noticed in some neurons of the frontal, parietal, and occipital cortices.<sup>64</sup> Compared with old-world monkeys and new-world monkeys, mouse lemurs exhibit more consistent Tau, p-Tau, and A $\beta$  depositions during aging, but rarely develop severe PHFs or NFTs.

In addition to rhesus monkeys, cynomolgus monkeys, and mouse lemurs, p-Tau was briefly studied in vervet monkeys, common marmosets, and tree shrews. A cohort of nine middle-aged vervet monkeys (11.2 years old in average) and nine aged vervet monkeys (21.7 years old in average) all exhibited A $\beta$  and Tau proteopathies in their brains.<sup>75</sup> A $\beta$  plaques were detected throughout the cortex in all aged vervets and in one middle-aged vervet, resembling early Braak staging in AD.<sup>75</sup> Intracellular PHF<sup>+</sup> p-Tau was detected in small cells with granular morphology in all monkeys, but NFTs were rarely observed.<sup>75</sup> Interestingly, higher levels of PHF<sup>+</sup> p-Tau was associated with slower gait speed, suggesting poorer integration of complex cognitive and motor processes and potential cognitive deficits.<sup>75</sup> Brain atrophy was associated with both the level of p-Tau in parenchyma and the level of Tau phosphorylated at threonine 181 (p-Tau181P).<sup>75</sup> This study demonstrated widespread A $\beta$  depositions, limited p-Tau aggregation, Tau-associated cognitive decline, and potential brain atrophy during the natural aging of vervet monkeys. Although none of these features meet the severity level observed in human AD, vervet monkeys may be a good NHP model recapitulating most cardinal features of AD. The common marmoset (*Callithrix jacchus*) is becoming an increasingly popular NHP model of AD due to its small body size (10–12 cm), small body weight (80–100 g), multiple births, and short life span (7–17 years).<sup>20</sup> Among male marmosets (1.6–18 years old), p-Tau was detected in their medial temporal areas and parietal cortices, and the level of Tau phosphorylated at threonine 231 (p-Tau231P) was positively associated with age.<sup>76</sup> By using Alz50, early fibrillary aggregation of p-Tau was detected in cytoplasmic compartments of neurons and glia-like cells in adolescent and aged marmosets.<sup>76</sup> Aged marmosets presented fewer active microglia but more dystrophic microglia in the dentate gyrus.<sup>76</sup> Hyperphosphorylation and conformational changes to Tau were exclusively detected in the dystrophic microglia.<sup>76</sup> Although extensive NFTs are not observed in marmosets, they still seem to be a valuable NHP model that demonstrates some features of human AD. Lastly, only one very recent study demonstrated Tau hyperphosphorylation in aged tree shrews, including adult tree shrews (3.8 years old in average) and aged tree shrews (6–7.5 years old).<sup>77</sup> As assessed by AT100, Tau hyperphosphorylation was significantly elevated in the dentate gyrus, the CA3 hippocampal region, and the subcortical structures of aged tree shrews in the absence of NFTs.<sup>77</sup> These aged tree shrews carried a higher number of IBA1<sup>+</sup> active microglia containing ferritin as well as microglia with a dystrophic phenotype.<sup>77</sup> Although not widely studied, tree shrews presented similar parenchymal A $\beta$  plaques, vascular A $\beta$  depositions,

Tau hyperphosphorylation, and microglial activation compared to human AD, indicating its potential suitability as a NHP model for translational research in AD.

### **Brain atrophy/neurodegeneration in aged NHPs**

The brains of naturally aging NHPs resemble human AD in many aspects, but the macroscopic feature of human AD, brain atrophy, is inconsistently observed. Using an optical fractionator technique, a preservation of neurons was observed in the subiculum, entorhinal cortex layer II, CA1, CA2, CA3, hilus, and the dentate gyrus of the hippocampal formation in aged rhesus monkeys.<sup>78,79</sup> In mouse lemurs, 20% of the elderly ( $\geq 5$  years old) demonstrated neurodegeneration.<sup>46</sup> Remarkable brain atrophy was observed in the cortex, corpus callosum, fornix, hippocampus, septum, thalamus, hypothalamus, basal ganglia, brainstem, and cerebellum, accompanied with ventricle dilatation, intensive parenchymal A $\beta$  plaques, and neurons with p-Tau.<sup>43,46</sup> Very recently, the number of neurons in CA1 and CA3 hippocampal subfields of chimpanzees were found to be negatively associated with advanced aging but not with AD pathologies.<sup>80</sup> In vervet monkeys, their cortical grey matter volume and temporal-parietal cortical thickness was negatively associated with age, potentially increasing the risk of cognitive decline.<sup>81</sup> In general, naturally aging NHPs demonstrate human-AD resembling proteopathies, glial activation, but severe brain atrophy and cognitive decline is rarely observed, striking our interest into the protective mechanism preventing severe demented symptoms from occurring.

### **Advantages and disadvantages of spontaneous NHP model of AD**

This chapter has elaborated the past and current findings of human AD-resembling pathologies in aged NHPs, including rhesus monkeys, cynomolgus monkeys, squirrel monkeys, and mouse lemurs (Table 2). Although species-to-species differences do exist, these species of NHPs demonstrate extensive A $\beta$  depositions in parenchyma and cerebral vessels, some degree of Tau and p-Tau depositions in parenchyma, rare intraneuronal accumulation of NFTs, glial cell activation, lemur-restricted brain atrophy, and mild cognitive deficits. Compared with other animal models of AD, naturally aging NHPs display high similarity to human AD because of their close phylogenetic relationship with humans, similar neuroanatomy, comparable genetics, and greater complexity in high-order cognitive functions.<sup>2,19</sup> Therefore, aging NHPs can be regarded as a promising model resembling AD that would improve our understanding of age-related cognitive impairment, disease-causing mechanisms, molecular and cellular interactions, and gene-environment interactions, further facilitating the development of diagnostic techniques and therapeutic innovations. Nevertheless, spontaneous NHP models of AD carry a few major limitations. Firstly, although naturally aging NHPs spontaneously demonstrate A $\beta$  proteopathies, they rarely exhibit AD-like NFTs or brain atrophy, suggesting some difficulty in using aged NHPs to analyse the interaction between A $\beta$ , Tau, and neuronal death. Secondly, cognitive deficits and executive function impairments in aged NHPs are much milder than those in human AD, which may be an obstacle to assess the performance of novel therapeutic treatments. It is interesting to study their protective mechanisms against severe NFTs, brain atrophy, and cognitive decline, while they display severe A $\beta$  proteopathies and ApoE  $\epsilon 4$  homozygosity. Lastly, NHPs usually have a long-life expectancy, compared with rodent models of AD, suggesting a longer inoculation period before AD-resembling symptoms thus adding to already high costs.

These disadvantages limit the broad use of naturally aging NHPs as spontaneous AD models.<sup>20</sup>

### **Induced NHP models of AD**

#### **A $\beta$ oligomer (A $\beta$ o)-induced NHP models of AD**

To overcome the disadvantages of spontaneous NHP models of AD, researchers injected A $\beta$  oligomers or fibrils into the brains of rhesus monkeys and cynomolgus monkeys, to establish an induced NHP model of AD. Synthetic soluble A $\beta$  peptides were first injected into multiple neocortical sites of rhesus monkeys (4–5 years old), but no AD-resembling cellular changes were noticed, although this may be caused by the short inoculation time or the solubility of the A $\beta$ .<sup>82,83</sup> The microinjection of plaque-equivalent A $\beta_{1-40}$  and A $\beta_{1-42}$  fibrils into the cerebral cortex of aged rhesus monkeys (25–28 years) resulted in diffuse A $\beta$  depositions with dense cores, clusters of dystrophic neurites, profound neuronal loss, intensive Tau phosphorylation, and microglia proliferation surrounding the injection sites.<sup>84</sup> These AD-resembling pathological alterations are associated with age as fibrillar A $\beta$  injection into young rhesus monkeys (5 years old) caused milder alterations.<sup>84</sup> In 2010, an induced NHP model of AD was established in middle aged rhesus monkeys (16–17 years old) via intracranial injection of A $\beta_{1-42}$  and thiorphan, which inhibited A $\beta$  clearance.<sup>85</sup> A $\beta_{1-42}$ /thiorphan-treated NHPs exhibited more significant intracellular A $\beta_{1-42}$  accumulation, cholinergic neuronal loss and atrophy, and microglia and astrocyte infiltration into the basal ganglia, cortex, and hippocampus of rhesus monkeys, compared with control monkeys.<sup>85</sup> However, they failed to show working memory deficits in DR tasks, possibly due to a short inoculation time of seven weeks.<sup>85</sup> Very recently, Beckman and colleagues conducted a more comprehensive study. A $\beta$ o was infused into the lateral ventricles of four female rhesus monkeys to compare with another two monkeys injected with scrambled A $\beta$  peptides and three age-matched female controls (11–19 years old).<sup>86</sup> Repeated A $\beta$ o injections resulted in A $\beta$  depositions near the pyramidal neurons in the dorsolateral prefrontal cortex and reductions in spine density in the apical and basal dendrites in A $\beta$ o-treated NHPs exclusively, indicating A $\beta$ o-induced interrupted synaptic integrity.<sup>86</sup> The volume of microglia in A $\beta$ o-treated monkeys were enlarged in the dorsolateral prefrontal cortices, in which active engulfment of synaptic markers by these microglia were noticed.<sup>86</sup> In the dentate gyrus of A $\beta$ o-treated monkeys, an increased number of rounded, amoeboid, and IBA-1<sup>+</sup> microglia were noted, suggesting altered innate immune responses induced by A $\beta$  oligomers.<sup>86</sup> TNF- $\alpha$  levels in cerebrospinal fluid (CSF) were also elevated in A $\beta$ o-treated monkeys that were associated with an increase in microglial activation in the dorsolateral prefrontal cortex, but no there were no detectable changes in Tau phosphorylation and neurofilament light levels.<sup>86</sup> In these studies, both soluble and insoluble A $\beta$ o or fibrils were used to establish the induced NHP models of AD and the administration of insoluble A $\beta$  fibrils is more likely to generate Tau phosphorylation and neuronal atrophy in rhesus monkeys, which better replicates the pathogenesis observed in human AD cases. Only one study examined memory deficits after A $\beta$ o injection and no deterioration in working memory was seen. In future studies, a longer injection period of A $\beta$ o, a longer inoculation period, and more cognitive examinations are expected to validate whether A $\beta$ o-treated rhesus monkeys can be used as an appropriate NHP model of AD.<sup>87</sup>

Unlike the extensive investigations into rhesus monkeys, the investigations into induced models of AD using cynomolgus



Table 2. Spontaneous (naturally aging) and induced NHP models of AD

Model types	Rhesus macaques	Cynomolgus monkeys	Squirrel monkeys	Mouse lemurs	Tree shrews
Spontaneous model					
Aβ plaques	AD-resembling burden level and distribution of Aβ plaques; more Aβ <sub>1-40</sub> than Aβ <sub>1-42</sub>	More Aβ <sub>1-40</sub> than Aβ <sub>1-42</sub> ; smaller Aβ plaques compared with human	Higher CAA burden than Aβ plaques	More Aβ <sub>1-42</sub> than Aβ <sub>1-40</sub> in Aβ plaques	Inconsistent results
CAA	Lower CAA burden than Aβ plaques			Extensive CAA with high Aβ <sub>1-40</sub>	Inconsistent results
Tauopathy	Rare AT8 <sup>+</sup> p-Tau; NFTs in the oldest old	rare AT8 <sup>+</sup> p-Tau in the oldest old		Age-associated p-Tau accumulations	Rare p-Tau
Neuronal death	–	–	–	20% of elderly demonstrated brain atrophy	–
Genetics (compared to human)	APOE ε4 monomorphism	identical APP <sub>695</sub> ; similar APP <sub>751</sub> & APP <sub>700</sub> ; APOE ε4 monomorphism	–	Identical APP exon 16 & 17; similar PSEN1 & PSEN2; APOE ε4 monomorphism	Similar APP & PSEN2; APOE ε4 monomorphism
Induced model					
Aβo-induced	Aβ, glial activation, p-Tau, memory deficits	Aβ, p-Tau, NFTs, glial activation, brain atrophy	–	–	Aβ, NFTs, brain atrophy, cognitive deficits
AD brain homogenate-induced	–	–	–	Aβ, p-Tau, NFTs, brain atrophy, memory and learning deficits	Aβ, p-Tau
STZ-induced	–	Aβ, p-Tau, glial activation, brain atrophy	–	–	–
FA-induced	Memory decline, Aβ, p-Tau, glial activation, p-Tau	–	–	–	–

AD, Alzheimer's disease; APOE, apolipoprotein E; APOE, apolipoprotein E; APP, amyloid precursor protein; CAA, cerebral amyloid angiopathy; NFT, neurofibrillary tangles; NHP, non-human primate; PSEN1, presenilin 1; PSEN2, presenilin 2.

monkeys only began in the past ten years. A well-known study conducted by Forny-Germano and colleagues injected synthetic A $\beta_{1-42}$  oligomers into the brains of four female cynomolgus monkeys compared with three sham animals.<sup>88</sup> The monkeys were younger than expected to naturally develop AD-resembling pathologies and symptoms.<sup>88</sup> The intracerebroventricular administration of A $\beta$  (ICV-A $\beta$ ) resulted in dense A $\beta$  accumulation in the entorhinal cortex, hippocampus (dentate gyrus), striatum, and amygdala, but little A $\beta$  accumulation in the midbrain or cerebellum.<sup>88</sup> Of note, whether A $\beta$  distribution was caused by the diffusion of solution or the propagation of disease-causing mechanism remains unknown.<sup>89</sup> Tau hyperphosphorylation at serine residue 396, an AD-specific epitope, was also induced in all regions with A $\beta$  accumulation in the brains of ICV-A $\beta$ -treated monkeys. Compared with sham-operated monkeys, Tau phosphorylation in ICV-A $\beta$ -treated monkeys was significantly higher.<sup>88</sup> The detection of high molecular mass p-Tau (>180 kDa) and low molecular mass p-Tau (<20 kDa) suggested Tau aggregates or oligomers, and truncated small Tau fragments in NFTs, respectively.<sup>88</sup> P-Tau, characterised by early phosphorylation markers, was detected in the brains of ICV-A $\beta$ -treated monkeys, as stained using AT100 and CP13 antibodies that recognised Tau phosphorylated at serine residue 212 and threonine residue 214, and at serine residue 202, respectively.<sup>88</sup> NFTs were also investigated using thioflavin-S staining, Alz59, and PHF-1, and their positive signals were detected in the neocortex of ICV-A $\beta$ -treated monkeys, resembling the distribution pattern of Tau tangles in human AD.<sup>88</sup> Regarding glial activation, a higher number of GFAP<sup>+</sup> astrocytes and IBA-1<sup>+</sup> microglia were noted in the frontal cortex, hippocampus, and amygdala of ICV-A $\beta$ -treated monkeys compared with those of sham monkeys.<sup>88</sup> Furthermore, synapse numbers, presynaptic and postsynaptic proteins, and synaptic puncta numbers were all decreased in ICV-A $\beta$ -treated monkeys, compared with controls, while A $\beta$ -induced apoptosis was not observed.<sup>88</sup> In brief, this study successfully demonstrated an ICV-A $\beta$ -induced NHP model of AD that recapitulated cardinal neuropathologies of AD except brain atrophy and behavioural alterations (behavioural alterations were not assessed in this study). The efficiency of this model is remarkable because cynomolgus monkeys only received one A $\beta$  injection every three days for up to 24 days and they were sedated only one week after treatment.<sup>88</sup> If experimenters allowed more time for inoculation, brain atrophy, learning decline, memory deficits, and behavioural alterations may be observed, alerting future studies to investigate NHP in a more comprehensive way. In 2021, a new injection method was proposed: bilateral injection of soluble A $\beta$  into the cerebral parenchyma of seven cynomolgus monkeys (~20 years old).<sup>90</sup> The authors prolonged the injection process into four injections over five months, followed by an eight-month inoculation before examination.<sup>90</sup> Using 6E10, 4G8, silver, thioflavin-S, and Congo Red staining, A $\beta$  plaques were found throughout the grey matter of limbic structures and the association cortex, accompanied by dense cores, in A $\beta$ -treated monkeys.<sup>90</sup> Intracellular NFTs reactive with AT8 and AT100 were also detected in neurons and astrocytes, and their morphological features resembled those observed in human AD, illustrating the co-existence of A $\beta$  and Tau proteopathies exclusively in A $\beta$ -treated monkeys.<sup>90</sup> Astrocytic and microglial activation surrounding A $\beta$  plaques were also noted, in which the inflammasome/caspase-1 signal was also activated and associated with A $\beta$  and Tau lesions.<sup>90</sup> Most importantly, the signals of neurodegeneration and the expressions of necroptotic cell death markers were detected in A $\beta$ -treated monkeys, while the density and intensity of presynaptic markers and the number of

basal forebrain cholinergic neurons were reduced.<sup>90</sup> In this study, the elevation of A $\beta$  dosage, injection period, and inoculation procedures resulted in potential neuronal loss and brain atrophy in A $\beta$ -treated monkeys, in addition to those cardinal AD features previously established in the Forny-Germano study. These two well-designed studies used ICV and intraparenchymal delivery methods of synthetic A $\beta$  and presented comprehensive characterisations of cynomolgus monkeys as the induced-NHP models of AD, including AD proteopathies, innate immune activation, indicative neuronal loss, and potential brain atrophy. They provided novel insights into future studies using increasing dosages, injections, and inoculation times are necessary to visualise Tau pathology and further increase the possibility of observing brain atrophy and behavioural alterations in NHPs.

Both ICV and intrathecal administration of A $\beta$  (IT-A $\beta$ ) into the brains of vervet monkeys has been reported to build an induced vervet model of AD.<sup>91</sup> Vervet monkeys received IT-A $\beta$  1–3 times a week for four weeks and were terminated at 1, 4, or 12 weeks after the last dose.<sup>91</sup> ICV-A $\beta$ -treated vervets exhibited higher levels of p-Tau, but all other AD-related pathologies were not assessed.<sup>91</sup> IT-A $\beta$ -treated vervets also demonstrated more intensive p-Tau signal as granular cytoplasmic staining in the perikaryal, fibres in the hippocampus, the dentate gyrus, the entorhinal cortex, and the subiculum.<sup>91</sup> 6E10<sup>+</sup> diffuse A $\beta$  depositions, IBA-1<sup>+</sup> microglia, and GFAP<sup>+</sup> astrocytes were all increased in IT-A $\beta$ -treated vervets compared with vehicle-treated vervets.<sup>91</sup> Most strikingly, significant reductions in hippocampal volumes were observed in IT-A $\beta$ -treated vervets that were terminated at four weeks after A $\beta$  administration, suggesting an acute, visible brain atrophy that was rarely observed in either spontaneous or induced NHP model of AD.<sup>91</sup> However, this study did not assess the biological components and conformational alterations of proteopathies, the morphological changes or activation of microglia and astrocytes, the pro-inflammatory profile in the vervet brain, and, most importantly, the behavioural alterations after IT-A $\beta$  injections.

In a study of tree shrews, 12 adult males were administered ICV-A $\beta$  (A $\beta_{1-40}$  peptides) and compared against six controls, followed by four-week inoculation period before brain imaging, histochemical examinations, and genetic analyses.<sup>92</sup> As expected, A $\beta$  burden, neuritic plaques, and NFTs were detected exclusively in the brains of ICV-A $\beta$ -treated tree shrews.<sup>92</sup> At four weeks post-injection, the hippocampal areas, the thickness of cells and the size of cells in the CA3 and the dentate gyrus of the ICV-A $\beta$ -treated tree shrews were significantly reduced, compared with untreated tree shrews.<sup>92</sup> The apoptosis assay further revealed an increased number of TUNEL<sup>+</sup> cells in the hippocampus, particularly in the dentate gyrus, of the ICV-A $\beta$ -treated tree shrews exclusively, indicating hippocampal atrophy.<sup>92</sup> ICV-A $\beta$ -treated tree shrews spent more time finding food at four weeks post-injection, reflecting altered hippocampal functions.<sup>92</sup> This study first screened differentially expressed genes between ICV-A $\beta$ -treated and control tree shrews at four weeks post-injection and identified downregulated BCL-2/BCL-XL-associated death promoter, inhibitor of apoptosis protein, and cytochrome C, as well as upregulated tumour necrosis factor receptor 1 in AD pathways.<sup>92</sup> These apoptosis-related gene alterations may explain brain atrophy in ICV-A $\beta$ -treated tree shrews. This study established an ICV-A $\beta$ -induced NHP model of AD that comprehensively examined AD proteopathies, brain atrophy, glial activation, and cognitive functions. The genetic analyses further elucidated the potential underlying mechanisms of brain atrophy. Strong evidence supports the idea that A $\beta$ -induced tree shrews can be a good NHP model of AD, but more sophisticated

examinations of their behavioural alterations are needed.

Collectively, injecting ICV-A $\beta$  and IT-A $\beta$  into the brains of NHPs can be efficient at inducing an NHP model of AD that recapitulates most of the cardinal features of human AD. It is beneficial for the study of A $\beta$ -associated consequences, particularly given the central role of A $\beta$  in AD pathogenesis. However, high doses of A $\beta$ , the precision of the surgery, and extensive inoculation time all make it challenging and expensive to build a stable A $\beta$ -induced NHP model of AD.<sup>20</sup> A significant gap in knowledge shared by most of the current studies is the lack of behavioural assessments due to incomplete study design or short inoculation period before termination that may limit the manifestation of any cognitive changes. Future studies are necessary to prolong the injection period and inoculation period, and allow for the incorporation of behavioural assessments that evaluate the suitability of A $\beta$ -induced NHP model of AD.

### **Brain homogenate-induced NHP models of AD**

The concept of a NHP model of AD induced by intracerebral injection of affected brain material has also been proposed. A total of 33 marmosets received an intracerebral injection of cerebral homogenates that were sourced from patients diagnosed with AD, other types of dementia, or myocardial infarctions as a control.<sup>93</sup> These marmosets were terminated once they showed neurological signs or survived 4.5–6.5 years if they did not manifest behavioural abnormality.<sup>93</sup> Among the AD brain homogenate-treated marmosets (6–7 years old), widespread A $\beta$  plaques, dystrophic neurites, and CAA were observed, but no NFTs or brain atrophy were detected.<sup>93</sup> Similar results were obtained in later studies, demonstrating that A $\beta$  or other associated factors can initiate and accelerate A $\beta$  deposition in parenchyma and cerebral vessels in marmosets but may not induce Tau pathology, glial activation, or neuronal death.<sup>94,95</sup> Moreover, 12 mouse lemurs were bilaterally inoculated with brain extracts from patients with AD, leading to widespread A $\beta$  and Tau proteopathies after 21-month inoculation period.<sup>96</sup> In AD brain homogenate-treated lemurs, diffuse A $\beta$  plaques, classical A $\beta$  plaques, and CAA were detected throughout the brain, accompanied by Tau proteopathy stained by AT8, AT100, and anti-pS422 antibodies.<sup>96</sup> AT8<sup>+</sup> NFTs or NFT-resembling p-Tau accumulations were localised around the inoculation sites (posterior cingulate cortex) along with the hippocampal and temporal areas.<sup>96</sup> This study successfully observed slight brain atrophy in the posterior cingulate cortex of AD-inoculated lemurs at 0–4 months and 9–15 months post-inoculation.<sup>96</sup> Simultaneously, AD brain homogenate-treated lemurs exhibited impaired learning abilities and impaired long-term memory performance compared with control lemurs, although their motor function remained intact.<sup>96</sup> For the first time in primates, this study demonstrated a comprehensive NHP model of AD that recapitulated major AD-associated proteopathies along with cognitive deficits and brain atrophy, highlighting the importance of long inoculation periods in experimental design. Of note, the severity of NFTs, brain atrophy, and behavioural abnormalities are still milder in AD brain homogenate-treated lemurs compared with humans diagnosed with AD.

### **Streptozotocin (STZ)-induced NHP models of AD**

STZ is a glucosamine-nitrosourea compound with a molecular weight of 265 Da, which was originally identified as an antibiotic with antimicrobial and antitumour effects.<sup>20,97</sup> The ICV injection of STZ (ICV-STZ) disrupts the phosphorylation of insulin receptors and blocks the insulin signalling pathway, leading to cholinergic impairments in the nervous system and compromised cog-

niton and memory, mimicking the insulin resistant brain state in human AD.<sup>20</sup> ICV-STZ and intraperitoneal injections of STZ can further degrade enzymes responsible for A $\beta$  clearance, promote A $\beta$  and Tau aggregation, glucose hypometabolism, oxidative stresses, and neurodegeneration.<sup>20,97</sup> STZ has been previously injected into transgenic mice to build animal models of AD, suggesting their potential use in inducing NHP models of AD.<sup>97</sup> Two cynomolgus monkeys (3 years old) received ICV-STZ (2 mg/kg) at the cerebellomedullary cistern 3 times on day 1, 7, and 14, and compared with two cynomolgus monkeys receiving normal saline.<sup>98</sup> In the ICV-STZ-treated monkeys, increased sulcal markings were observed using magnetic resonance imaging (MRI) 6 weeks after the first ICV-STZ injection, suggesting immediate diffuse brain atrophy, but these structural changes were resolved at 12 weeks post-injection.<sup>98</sup> [<sup>18</sup>F]-FDG-PET was used to characterise glucose metabolism in this model and revealed glucose hypometabolism in the precuneus, posterior cingulate, and medial temporal areas in ICV-STZ-treated monkeys, which resembled the distributive pattern of glucose hypometabolism in early AD patients.<sup>98</sup> This same group subsequently used the same experimental design to investigate molecular changes induced by ICV-STZ in female cynomolgus monkeys (3 years old). The mRNA expression of insulin-related genes was altered in the anterior part of the cerebrum, frontal cortex, and hippocampus, which resembled these areas of the brain in patients with early AD.<sup>99</sup> Subsequently, ICV-STZ-treated cynomolgus monkeys were used to characterise the profile of 7 APP processing-related genes (ADAM10, ADAM17, BACE1, PSEN2, NCSTN, APH1A, and PSENEN) and five Tau phosphorylation-related genes (CDK5, CDK5R1, CAPN1, AKT1, and GSK3 $\beta$ ).<sup>100</sup> In ICV-STZ-treated monkeys, mRNA levels of ADAM10, ADAM17, PSEN2, PSENEN, NCSTN, and APH1A were significantly upregulated 1.6–2.1 fold in the precuneus and occipital cortex compared with control monkeys, while BACE1 upregulation was only observed in the occipital cortex.<sup>100</sup> Downregulation of ADAM17 and upregulation of PSENEN and NCSTN were observed in the frontal cortex.<sup>100</sup> The Tau-associated genes, CDK5R1, CAPN1, and GSK3 $\beta$  were significantly upregulated in the precuneus and occipital cortex.<sup>100</sup> ICV-STZ treatment generally resulted in higher transcription levels of APP processing and Tau phosphorylation-related genes in the frontal and occipital cortices, except CDK5, indicating that these genes might be simultaneously regulated in specific regions.<sup>100</sup> In a later study, 6 cynomolgus monkeys (5–8 years old) were used to assess ICV-STZ-induced AD-resembling features.<sup>101</sup> Half of the monkeys were administered 4 doses of STZ (2 mg/kg) via the cerebellomedullary cistern on weeks 0, 1, 2, and 28, while the other half of the cohort were injected with artificial CSF.<sup>101</sup> Monkeys were terminated 36 weeks after the first dose of ICV-STZ, which was equivalent to 8 weeks after the final dose of ICV-STZ.<sup>101</sup> ICV-STZ-treated monkeys exhibited prominent A $\beta$  plaques with dense core in the parenchyma of the temporal cortex and dense CAA in microvessels in the insular cortex, while the brains of control monkeys illustrated minimal or no A $\beta$  immunoreactivity, approximately four-fold different as quantified using immunostaining.<sup>101</sup> In the temporal cortex and hippocampus, p-Tau was detected in the neuronal cytoplasm as tangles and straight fragments, accompanied by severe cell loss, atrophy, and morphological alterations.<sup>101</sup> Within the ventricular wall and the periventricular area, densely stained GFAP<sup>+</sup> astrocytic fibres and numerous IBA-1<sup>+</sup> microglia/macrophages with amoeboid morphology were observed in ICV-STZ-treated monkeys, indicating astrogliosis, microglial activation, and inflammatory processes.<sup>101</sup> This study was the first ICV-STZ study that comprehensively assessed

the histology of the brain in these monkeys and demonstrated an induced model that resembled AD. Interestingly, monkeys that received 3 ICV-STZ injections did not display structural changes at week 24, but monkeys that received 4 ICV-STZ injections on week 28 displayed ventricular enlargement and parenchymal atrophy at weeks 30, 32, and 34.<sup>101</sup> The first three doses of ICV-STZ may make the brain more susceptible to cerebral damage and additional doses may be needed to induce remarkable brain atrophy, further illustrating the importance of dose and inoculation time in NHP studies. To date, only one study has comprehensively assessed the microscopic and macroscopic features of ICV-STZ-treated monkeys, and no study has evaluated ICV-STZ-induced cognitive decline and behavioural changes yet. Of note, the surgical procedures used in this method may cause penetration injuries that would affect the general theoretical basis of the model.<sup>20</sup> Considering these limitations, more studies are needed to strengthen the validity of this model.

### Formaldehyde (FA)-induced NHP models of AD

AD is a complicated disorder that is determined by both genetic and environmental risk factors, including air pollution, heat waves, heavy metals, and others. For instance, long-term exposure to environmental lead led to elevated expression of AD-related genes and transcriptional regulators (Sp1), decreased DNA methyltransferase activity, and increased DNA oxidative damage in aged cynomolgus monkey.<sup>102</sup> FA is a highly reactive single-carbon aldehyde that is widely distributed in living organisms (intrinsic FA) and the environment (extrinsic FA).<sup>20,103</sup> Endogenous FA is the by-product of aldehyde metabolism sourced from the oxidation of methanol, histone demethylation, and methylamine deamination.<sup>103</sup> FA has been classified as a carcinogen and teratogen by the World Health Organisation.<sup>20</sup> It is known to damage the balance of neurotransmitters, influence long-term potentiation in the hippocampus, and influence DNA methylation that may eventually lead to memory decline.<sup>20</sup> In AD, patients intrinsically accumulate excessive FA which then induces A $\beta$  aggregation, Tau hyperphosphorylation and fibrillation, neuronal loss, memory impairment, and learning deficits.<sup>103</sup> In Yang *et al*, 4 male rhesus monkeys (3–4 years old) were chronically fed with 3% methanol *ad libitum* and compared with nine control monkeys to study the chronic effects of methanol exposure.<sup>104</sup> After the variable spatial delay response task was performed, two methanol-treated monkeys experienced persistent memory decline that lasted 6 months after the feeding regimen.<sup>104</sup> Meanwhile, approximately 1.25 years into this study, the level of p-Tau in CSF was dramatically higher in methanol-treated monkeys compared with the control monkeys.<sup>104</sup> A $\beta$  plaques and p-Tau were identified in the parietal, temporal, frontal lobes, and the hippocampus of methanol-treated monkeys exclusively.<sup>104</sup> This study investigated the chronic effects of methanol and its FA metabolite in AD, but its results were limited by its small sample size and inconsistent study design for each rhesus monkeys. In the following study, young rhesus monkeys (5–8 years old) were administered with ICV-FA injections over 12 months to study FA-induced effects.<sup>105</sup> ICV-FA-treated monkeys exhibited A $\beta$  plaques, neuritic-like plaques, NFT-like formations, higher level of p-Tau, neuronal loss, and activated astrocytes and microglia in their hippocampus, entorhinal cortex, and prefrontal cortex, compared with controls.<sup>105</sup> Similarly, ICV-FA-treated monkeys illustrated significant spatial working memory impairments.<sup>105</sup> In these two studies of FA-induced NHP models of AD, FA-treated NHPs demonstrated consistent A $\beta$  depositions, Tau hyperphosphorylation, and memory impairment. Nevertheless, the method of methanol feeding

requires modification as methanol itself is associated with side effects that are hard to distinguish based on histological examination and behaviour assessment.<sup>20</sup>

### Advantages and disadvantages of induced NHP models of AD

This chapter has discussed current studies that used ICV-A $\beta$ , IT-A $\beta$ , AD brain homogenate, ICV-STZ, methanol, and ICV-FA to induce NHP models of AD (Table 2). Aged NHPs share great similarities with human, including neuroanatomy, neurophysiology, complicated behaviours, and complex emotions, making them ideal models for human disorders. The application of A $\beta$ , AD brain homogenate, STZ, and FA further fills the gap between naturally ageing NHPs and human with AD by inducing Tau hyperphosphorylation, potential fibrillation of p-Tau, neuronal loss, brain atrophy, cognitive decline, and memory impairment. Most importantly, the injection or feeding of AD-associated inducers allow the emergence of AD-associated pathologies and behaviours at the young adult age in NHPs rather than at the elder age in naturally aged NHPs, which greatly limits financial needs and shortens experimental procedures. Nevertheless, all current modelling methods are associated with limitations. First, the dose, injection period, and inoculation period vary between studies and the procedures have not been standardised. Studying two well-designed A $\beta$ -induced NHP studies, increasing the dosage, prolonging the injection period, and extending the inoculation period up to two years may allow NHPs to develop all AD-resembling pathologies and symptoms, most importantly, brain atrophy and cognitive decline.<sup>88,90</sup> The occurrence of brain atrophy and cognitive decline is hardly observed in spontaneous NHP models of AD, but they are severely affected in patients with AD, suggesting their importance in therapeutic development and validation in AD models. Secondly, the study design of constructing an induced NHP model of AD awaits great improvement. Many studies only included two or three NHPs in the treatment group, so the presentation of AD-resembling pathologies may be a result of chance. A more comprehensive assessments of induced NHPs is encouraged, including the examinations of A $\beta$  plaques, CAA, p-Tau, NFTs, glial activation, inflammatory profile, neuronal death, brain atrophy, and behavioural changes. A more standardised evaluation of NHP models will contribute to better communication between studies, making the ultimate use of time and capital in each study, and leading to more efficient construction of a well-recognised standardised NHP model of AD. In addition, given the incomplete understanding of AD aetiology, all artificially induced models are based on a specific hypothesis of AD, making it hard for one NHP model to fully recapitulate AD pathologies and symptoms.<sup>20</sup> Constructing such models should be one of the main focuses and obstacles in this field. More efforts are expected to improve methodology, increase consistency, and eventually standardise the protocol of induced NHP models of AD.

### Evaluation of NHP models of AD

While spontaneous and induced NHP models of AD are still being developed, the methods and techniques used to assess hallmarks of AD in these models must be standardised simultaneously. Most of the diagnostic techniques used in human AD studies and the behavioural tests used in rodent models of AD have been applied in NHP models of AD to evaluate disease pathology and treatment efficacy. Common clinical examinations include A $\beta$  PET scan, MRI, and electroencephalogram (EEG), while biofluid samples, such as CSF and plasma samples, are mainly used in laboratory tests. Various behavioural and cognitive tests, which are specific to

NHP models of AD, have also been recently developed.

### Brain imaging

A $\beta$  PET scans are broadly used in clinical settings for AD diagnosis and increasingly used in NHP models of AD. The common tracer used in human studies, Pittsburgh Compound B (<sup>11</sup>C-PIB), is not suitable for use in aged rhesus monkeys, squirrel monkeys, or chimpanzees.<sup>106</sup> <sup>18</sup>F-Fluoroazabenzoxazoles (MK-3328), developed by Merck, has shown promising results for rhesus monkeys, which will be discussed in the next chapter.<sup>107</sup> Besides A $\beta$  PET scans, <sup>18</sup>F-ASEM which targets the nicotinic acetylcholine receptor has also been used in a NHP model.<sup>108</sup>

MRIs have also been used in NHP models of AD to evaluate disease progression. Gary and colleagues induced AD-like symptoms in 12 middle-aged mouse lemurs (~3.5 years old) by intracerebral injections of brain extracts from AD patients, followed by an 18-month inoculation and monitoring with a 7.0 Tesla spectrometer.<sup>109</sup> Progressive cerebral atrophy was observed.<sup>109</sup> MRI was also applied in middle-aged and aged vervet monkeys to investigate the associations between brain volumetrics and other AD markers.<sup>75</sup> Smaller MRI volumes in the right prefrontal, left inferior, and left posterior temporal cortex were found to be associated with higher levels of pTau-181 in CSF.<sup>75</sup> Similar age-related brain volume changes in young and old vervet monkeys were also reported using MRI.<sup>81</sup> Additionally, MRI has been used to examine amyloid-related imaging abnormalities, a potentially serious side effect in clinical trials for AD that is closely associated with CAA. Aged squirrel monkeys showed both edematous and hyperintense types of amyloid-related imaging abnormalities, accompanied by reactive astrocytosis, microgliosis, infiltration of systemic inflammatory/immune cells, damage to axons and myelin, and hemosiderin deposition.<sup>110</sup>

### EEG and electromyogram (EMG)

EEG and EMG are common clinical methods for monitoring brain function, but neither has been widely used in NHP models. Gary and colleagues applied EEG and EMG coupling analysis in their mouse lemur model of AD. Briefly, after inoculation with brain extracts from AD patients, slow wave EEG frequencies were observed with a lower delta frequency and a higher theta frequency in the experimental group, compared with the control-inoculated group.<sup>109</sup> New EEG devices designed specifically for rhesus monkeys have also been reported,<sup>111</sup> which could greatly facilitate the studies of NHP models.

### Laboratory tests

Many of the current clinical laboratory diagnostic methods have also been used in studies of NHP models of AD, including the CSF biomarker assay, cell biology examination, and histological staining. Chen and colleagues measured A $\beta$ <sub>1-40</sub>, A $\beta$ <sub>1-42</sub>, t-Tau, and P-Tau181P in 329 vervet monkeys and found similar changes in these biomarkers as in human AD patients.<sup>112</sup> Increased levels of FA in CSF were found in aged rhesus monkeys and the levels were negatively associated with the A $\beta$  burden.<sup>113</sup>

Immunohistochemical staining is broadly used in NHP models of AD. In a study comparing 6-month-old APP/PS1 mice, ~31-year-old rhesus monkeys, and ~86-year-old humans, mitochondrial clusters were found surrounding A $\beta$  plaques in all three species.<sup>114</sup> Larger particles of lipofuscin, a deposit of oxidised lipids and proteins, and greater plaque-associated astrocyte activation were found in the brains of monkeys and human participants. Extensive non-ramified microglia were also noticed.<sup>114</sup> T cell infiltration was found in the white matter of the parenchyma of the

aged monkeys,<sup>115</sup> resembling human AD. Other AD-resembling pathological characteristics, such as A $\beta$  plaques, dendritic spine loss, Tau, p-Tau, and activated astrocytes, were also found in NHP models of AD.<sup>86,109</sup> These data demonstrate similar pathological features shared by both aged NHP and human subjects.

### Behavioural tests

Monkeys have a rich behavioural repertoire that lends themselves as suitable for translational studies of human cognition.<sup>18</sup> Many behavioural tests have also been developed in NHP models.

#### Cognitive and learning tests

##### A computerised visuospatial learning task

After a stimulus is presented to a monkey, the computer screen becomes blank. Following a 2-s delay, three objects are presented. The monkey is expected to choose the original object. Usually 20 trials/session are presented over 20 consecutive sessions.<sup>116</sup>

##### Manual delayed match to position task

A test of working memory capacity in a Wisconsin General Testing Apparatus.<sup>29,85,117</sup> It assesses monkeys' ability to correctly identify the location of a food reward that they previously saw hidden, following various delays.<sup>115,118</sup>

##### DNMS task

A benchmark task of learning and recognition memory that measures a monkeys' ability to distinguish between a recently presented object and a novel object following a delay period of 10 s. Once this is learned, additional tests of recognition memory will be performed after delays of 2 mins and 10 mins. Outputs of the acquisition phase, 2-min delay phase, and 10-min delay phase are used as measurements of learning and recognition memory.<sup>115,119-121</sup>

##### Computerised delayed match to sample (DMTS) task

This task begins with a pre-training session known as "shaping procedures" followed by a DMTS trial. In the previous apparatus, colour choice selections are made by pressing clear push keys with light emitting diodes located behind them. The current apparatus is equipped with touch-sensitive computer monitors that presents the colour choices automatically.<sup>118</sup>

##### Circular platform test

Spatial performance is assessed in a circular platform apparatus, which is a modified version of the Barnes maze, specifically adapted for mouse lemurs.<sup>122,123</sup>

##### Visual discrimination test (mouse lemurs)

The cognition of mouse lemurs is evaluated in an apparatus adapted from the Lashley jumping stand apparatus, a vertical cage made of plywood walls, except for the front panel, which is a one-way mirror allowing observation. Two discrimination tasks are performed, a learning task and a long-term memory task. These tests involve a succession of visual discrimination tasks, during which the mouse lemur must jump from a heightened central platform to one of two lateral boards.<sup>109</sup> One of the boards allows access to a reinforcing chamber containing a positive reward (the possibility of reaching a safe nestbox for a 2-min rest).<sup>109</sup>

##### Touchscreen-based cognitive testing

Mouse lemurs are trained individually in customised, sound-attenuated Bussey-Saksida Touchscreen Chambers.<sup>124</sup> Lemurs receive

one training session per day. Each session lasts for a maximum duration of 30 (pre-training sessions) or 60 (sessions during actual cognitive testing) mins or until 30 trials have been completed by the respective subject. All lemurs are naïve to the touchscreen setup and must undertake a pre-training procedure before they begin the actual cognitive task. The pre-training procedure consists of five different stages (PT 1 to PT 5), during which the lemurs procedurally learn to interact with random, pictorial pre-training stimuli presented in one of two possible response windows on the touchscreen for a reward. The actual cognitive test, a pairwise discrimination/pairwise discrimination reversal, includes two fundamentally different stages: an initial, visual PD acquisition stage followed by a PDR procedure.<sup>51,124</sup>

#### T-maze

This test is designed based on earlier studies in rats and macaques and is scaled for the relative size of NHPs. Each monkey is introduced into the maze in a series of stages. Following pre-training, monkeys are trained on the spatial DNMS tasks. The monkey is only rewarded if it enters the correct choice arm. This learning phase continues for four trials/day, five days/week, until the animal achieves a criterion of 36 correct responses in 40 consecutive trials.<sup>125</sup>

#### DRST Object and Spatial

This tests monkeys' working memory capacities by requiring them to identify a new stimulus among an increasing array of serially presented, familiar stimuli using spatial and subsequent nonspatial (objects) stimuli. The span of correct responses across trials is a measurement of working memory.<sup>115,119</sup>

#### Conceptual set shifting task

This tests monkeys' executive function by requiring them to learn rules that are not explicitly learned. It resembles the Wisconsin Card Sorting Task: once a task is learned, the "rule" is switched, so that monkeys must shift to learn a new rule. The errors monkeys make, specifically the perseverative errors made after set shifting, is the measurement of executive function.<sup>115</sup>

#### Spatial reversal learning

A stimulus tray with three identical, equally spaced wells is used. The correct response is to displace the plaque on the positive side and obtain the food reward. The outcome measure is the total number of trials required for three sequential reversals.<sup>119,126</sup>

#### Inhibitory control of behaviour (squirrel monkeys)

The apparatus is a clear Plexiglas box with one open side baited with a treat. The box is locked into place on a horizontal tray secured to a tripod placed in front of each monkey's cage. After initial training, the box opening is oriented towards different directions, the direction of each reach attempt and the hand used on successful retrievals are recorded.<sup>127</sup>

### Motor function assays

#### Motor function assay

NHPs are placed on a platform. Distance travelled and movement speed are quantified for each NHP using a commercially available video-tracking system in accordance with the published procedures.<sup>128,129</sup>

#### Accelerating rotarod task (mouse lemurs)

Mouse lemurs are placed on a 5-cm-diameter rotating cylinder

turning at 20 rotations per minute (rpm). The rod then accelerates steadily up to 40 rpm until the end of the test, which is reached when the animal falls or grips onto the rod during at least three consecutive turns without stabilising its balance. Latency to fall off or grip the rod is recorded for each trial. Mouse lemurs will take five consecutive trials, and the best result is recorded with the values expressed in seconds.<sup>109</sup>

#### Gait speed (usual walking speed)

The time a NHP takes to traverse a minimum of three feet at a normal pace without provocation is recorded as its usual walking speed via stopwatch. The measurements of usual walking speed are conducted during the day (07:00–16:00 hours) over the course of a month before necropsy. A minimum of five valid instances are used to calculate the mean speed.<sup>75,130</sup>

### Applications of NHP models of AD:

#### *PET imaging and tracer validation*

Although the gold-standard diagnosis of AD is the post-mortem examination of A $\beta$  and Tau proteopathies, the field is currently evolving the diagnostic criteria into a suite of neuroimaging and fluid biomarkers to identify pre-clinical and prodromal patients with biomarker positivity before the onset of dementia symptoms. CSF measurements of A $\beta$  and Tau, and PET imaging of A $\beta$  burden are currently the most advanced and accurate diagnostic tools that are restricted in research settings and clinical trials. To further improve the diagnostic accuracy and sensitivity, developing various neuroimaging techniques and identifying AD-specific radiopharmaceuticals that allow the non-invasive appraisal of A $\beta$  or Tau lesions are encouraged.<sup>2</sup> Given the similarity of neuroanatomy, genetics, and protein homology between NHPs and humans, NHPs can make great contributions to the pre-clinical evolution of AD-associated radiopharmaceuticals regarding safe evaluation, kinetics mimicking, selectivity, and specificity assessments.<sup>2</sup> Four [<sup>18</sup>F]Fluoroazabenzoxazoles PET tracers, including [<sup>18</sup>F]MK-3328, [<sup>18</sup>F]AD-269, [<sup>18</sup>F]AD-278, and [<sup>18</sup>F]AD-265, were evaluated for their *in vitro* binding to human A $\beta$  plaques, lipophilicity, and blood-brain barrier permeability in rhesus monkeys.<sup>107</sup> [<sup>18</sup>F]MK-3328 illustrated the best combination of low *in vivo* binding potential in white matter and cortical grey matter, low lipophilicity, and high affinity for A $\beta$  plaques in rhesus monkeys.<sup>107</sup> [<sup>18</sup>F]MK-3328 was subsequently tested in AD patients, showing punctuate, displaceable binding in the cortical grey matter without binding in the cerebellum.<sup>107,131</sup> It was then tested in clinical trials among healthy controls and AD patients, but only fulfilled phase one until its premature termination.<sup>131</sup> NHP models can play a fundamental role in PET tracer development and safety evaluations, paving the road towards clinical trials involving human participants.  $\gamma$ -secretase modulators (GSM) and synthesised [<sup>11</sup>C]SGSM-15606 were developed to visualise the distribution of  $\gamma$ -secretase in one male rhesus monkey (13 years old).<sup>132</sup> This  $\gamma$ -secretase-based PET radioligand demonstrated high selectivity and high brain intake, in the midbrain and anterior cingulate cortex.<sup>132</sup> This study provides the first molecular neuroimaging of  $\gamma$ -secretase, which not only facilitates the investigation of the role of A $\beta$  and  $\gamma$ -secretase in AD pathogenesis, but also helps in drug assessment and development.<sup>133</sup> In addition to the development and validation of novel PET tracers using NHPs, some studies also use NHPs to evaluate the association between different tracers targeting A $\beta$  plaques, glucose metabolism, mitochondrial proteins, and acetylcholine

receptors, aimed at improving our understanding of AD pathogenesis.<sup>134,135</sup>

Beyond molecular neuroimaging of A $\beta$  plaques and A $\beta$ -related proteins, other studies have also evaluated novel PET tracers for neuroimaging of AD-associated proteins or receptors. <sup>11</sup>C-LSN3172176 was synthesised to visualise the M<sub>1</sub> muscarinic acetylcholine receptor (mAChR) in rhesus monkeys.<sup>136</sup> mAChR plays a critical role in learning and memory and is tightly associated with cognitive decline in neurological disorders, including AD.<sup>136</sup> <sup>11</sup>C-LSN3172176 displayed rapid metabolism, fast kinetics, and high uptake in the brains of rhesus monkeys, while its uptake was significantly reduced with pre-treatment with scopolamine and AZD6088.<sup>136</sup> The validity examination of <sup>11</sup>C-LSN3172176 in NHPs suggested that it may be the first optimal radiotracer for mAChR.<sup>137,138</sup> Furthermore, as dysregulation of microtubule is associated with AD, [<sup>11</sup>C]MPC-6827 was developed to image microtubules and assess reproducibility in male cynomolgus monkeys.<sup>139</sup> Soluble epoxide hydrolase is a bifunctional enzyme, and its dysregulation is associated with neuropathologic disorders, including AD.<sup>140</sup> A novel PET tracer for imaging soluble epoxide hydrolase, [18F]FNDP, was first tested in the brains of baboons and demonstrated high and rapid brain uptake.<sup>140</sup> Given the high similarities between NHPs and human, NHPs have become involved in the evaluation of novel AD-associated PET tracers to pave the way towards clinical translation in human subjects. NHP models of AD are more valuable than rodent models of AD in the pre-clinical assessment of neuroimaging biomarkers because they can resolve many concerns, including the safety, kinetics, sensitivity, and specificity of PET tracers, which reduces the cost of unnecessary clinical trials and increases the translational rate of novel PET tracers.

#### **Active immunotherapy (vaccination)**

Active immunotherapy, or preventative immunisation, uses inactivated virus, bacteria, or part of these pathogens to stimulate the patient's immune system to generate antibodies against the pathogen, such as against A $\beta$  in AD. A cocktail of human A $\beta$  peptides were injected into five aged vervet monkeys over 10 months, leading to the generation of plasma anti-A $\beta$  antibodies that could recognise monomeric and oligomeric A $\beta$  instead of full-length APP.<sup>141</sup> Immunisation with human A $\beta$  peptides also resulted in increased plasma levels of A $\beta$ <sub>1-40</sub> at day 300, accompanied by significantly lower levels of CSF A $\beta$ <sub>1-40</sub> and A $\beta$ <sub>1-42</sub> at day 100, suggesting the controversial "peripheral sink hypothesis".<sup>141</sup> Of note, all vervet monkeys recruited in this study already demonstrated severe A $\beta$  plaques and CAA prior to active immunisation, but the authors did not compare parenchymal and vascular A $\beta$  burden pre- and post-immunisation.<sup>141</sup> Active immunisation studies using NHPs should use young, disease-free NHPs to enable researchers to observe the effects of the vaccine. Subsequently, 25 young, disease-free mouse lemurs were used to observe antibody responses after immunisation with A $\beta$ <sub>1-42</sub> and its derivatives, including K6A $\beta$ <sub>1-30</sub>, K6A $\beta$ <sub>1-30</sub>[E<sub>18</sub>E<sub>19</sub>], and A $\beta$ <sub>1-30</sub>[E<sub>18</sub>E<sub>19</sub>].<sup>142</sup> K6A $\beta$ <sub>1-30</sub> resulted in high, stable anti-A $\beta$  IgG responses in multiple mouse lemurs, so researchers chose this derivative for further immunisation in older primates.<sup>142</sup> Cynomolgus monkeys were also immunised with the A $\beta$  vaccine combined with prior immunisation of a diphtheria-tetanus toxoid vaccine.<sup>143</sup> Very recently, optimised ACI-24, a liposome vaccine designed to generate anti-A $\beta$  antibody responses without simultaneous T cell activation, was also tested on young four cynomolgus monkeys in a pre-clinical study.<sup>144</sup> Vaccinated cynomolgus monkeys generated high levels of IgG antibodies

against pyroglutamate A $\beta$ .<sup>144</sup> These studies revealed several roles for NHPs in pre-clinical studies of AD vaccination, including vaccine tolerance, kinetic assessment, and long-term monitoring of side effects, aiding the translational application of AD vaccines in human subjects. Additionally, assessing whether an A $\beta$  vaccine can ameliorate AD-associated pathologies is critical. Multiple species of NHPs, including rhesus monkeys, cynomolgus monkeys, and pigtailed monkeys, were immunised using aggregated A $\beta$ <sub>1-42</sub> admixed with monophosphoryl lipid A as an adjuvant for five consecutive times within 14 weeks, followed by six-months of monitoring.<sup>145</sup> While all animals developed a strong, sustained level of anti-A $\beta$  IgG antibodies in serum, only 80% of the aged NHPs generated detectable antibodies and their immune responses were more delayed and weaker compared with the younger monkeys.<sup>145</sup> Comparing the pre- and post-immunisation levels of CSF A $\beta$  and Tau, slight decreases in CSF A $\beta$ <sub>1-42</sub>, increases in Tau, and differences in Tau/A $\beta$ <sub>1-42</sub> ratio were observed in the aged population.<sup>145</sup> Regarding the A $\beta$  burden at the pre- and post-immunisation stages, this study only compared histopathologic examinations in all immunised NHPs and non-immunised NHPs and they performed A $\beta$  PET scanning at baseline.<sup>145</sup> Overall, compared with rodent models of AD, NHPs are the superior models of AD that can accurately predict how long a vaccine will generate antibodies and how adverse effects will present in pre-clinical studies. The simultaneous use of a rodent model and NHP model are encouraged to obtain robust information prior to clinical trials involving human subjects.<sup>2</sup> In the last two decades, young and disease-free NHP models of AD have been mainly used to evaluate the safety and tolerance of AD vaccines in pre-clinical studies. In future studies, young, disease-free NHPs are expected to be examined by PET neuroimaging of A $\beta$  and Tau pre- and post-immunisation to estimate whether AD vaccines can prevent or post-pone the occurrence of AD pathologies before clinical trials.

#### **Therapeutic development and validation**

##### **Passive immunotherapy (mAb)**

The field has developed advanced techniques to identify patients at the asymptomatic phase for early management, aiming at postponing clinical symptoms or reversing pathogenetic mechanisms, but no DMTs have been granted expecting symptom-modifying treatments. The current symptom-modifying treatments of AD include inhibitors of acetylcholinesterase enzyme (AChE) (donepezil, galantamine, and rivastigmine) and N-methyl-D aspartate (NMDA) receptor antagonists (memantine).<sup>146</sup> Donepezil could ameliorate spatial cognition deficits and protect neurons from senility in an A $\beta$ -induced tree shrew model of AD,<sup>147</sup> while memantine has demonstrated partial effectiveness in resolving spatial memory impairment.<sup>123</sup> Given the improved understanding of AD in recent decades, some researchers advocate that AD may be caused by an impairment of innate immunity, and that it may be treated by tools of adaptive immunity.<sup>148</sup> The administration of anti-A $\beta$  and anti-Tau mAb might be effective passive immunotherapies of AD.<sup>146</sup> NHPs are rarely involved in the pre-clinical testing of mAb therapies. Only one study re-engineered a single chain Fv antibody against A $\beta$  with a fusion protein with mAb against the human insulin receptor to develop mAb-based therapy of AD that can cross the human blood-brain barrier.<sup>149</sup> Given the currently available spontaneous and induced NHP models of AD, essential pre-clinical studies involving NHPs are expected to test the safety, efficiency, and long-term adverse effects of mAb treatments of AD prior to the translation into clinical trials involving human subjects. The field is investigating numerous human resources and financial

investments into the clinical trials of mAb treatments, but its low translational rate is remarkable.<sup>146</sup> One possible explanation is that the human subjects recruited by clinical trials are already too old to be treated by mAb treatments. In addition to rodent models of AD, recruiting NHP models of AD at middle age in pre-clinical studies will contribute to identification of the effects of mAb treatments and selecting the most promising mAb treatments, facilitating further translational work with controlled budgets.

### AD pathogenesis-associated treatments

While anti-A $\beta$  or anti-Tau mAb treatments target the cardinal features of AD, AD is also associated with neuroprotective factors and many receptors that may have therapeutic potential. Pathological alterations in neuronal circuits and synapses may explain the link between AD proteopathies and cognitive impairment.<sup>150</sup> Brain-derived neurotrophic factor (BDNF) is tightly associated with neuronal survival in the entorhinal cortex and maintenance of synaptic plasticity in learning and memory.<sup>150</sup> In adult and aged rhesus monkeys, lentiviral vectors expressing BDNF genes were delivered into their entorhinal cortices.<sup>116</sup> BDNF prevented lesion-induced neuronal death in the entorhinal cortex, reversed neuronal size in the entorhinal cortex, and ameliorated age-related impairments in visuospatial cognition.<sup>116</sup> Based on these preliminary results, the first-in-human clinical trial that test whether AVV2-BDNF gene therapy will slow or prevent neuronal loss in the brains of patients with early AD will start shortly ([www.clinicaltrials.gov/ct2/show/NCT05040217](http://www.clinicaltrials.gov/ct2/show/NCT05040217)). Furthermore, the cholinergic system is also a critical focus of therapeutic development in AD, such as donepezil, one of the granted symptom-modifying treatments of AD. The fourth subtype of mAChR, M4, participates in the actions of acetylcholine and has become a new target to modify behavioural and cognitive alterations in AD.<sup>151</sup> Very recently, the effect of an M4 receptor was characterised in six adult rhesus monkeys.<sup>151</sup> This compound improved cognitive abilities in the object retrieval de-tour task and the visuospatial paired-associates learning, suggesting its potential in modifying AD symptoms.<sup>151</sup> However, whether this novel compound is superior to the existing AChE inhibitors for AD requires further investigation.

### Drug repurposing

The translation from laboratory discoveries into clinical applications of novel therapeutics takes substantial amounts of time and human resources in addition to being accompanied by a high failure rate. Thus, the repurposing of “old” drugs with approved safety, tolerance, and adverse effects to treat common and rare diseases is becoming a popular.<sup>152</sup> AD has long been associated with diabetes. A high sugar/high fat diet, physical inactivity, and mental stress all lead to hyperglycaemia, which is the main feature of insulin resistance and diabetes, further resulting in cognitive deterioration.<sup>153</sup> The brains of human subjects with AD are characterised by defective insulin signalling and impaired glucose metabolism, indicating that anti-diabetic treatments may be promising DMTs for AD.<sup>154</sup> In 2018, liraglutide, a glucagon-like peptide 1 analog developed to treat type 2 diabetes, was tested in A $\beta$ -induced NHP model of AD.<sup>154</sup> Based on the A $\beta$ -induced NHP protocol established by Forny-Germano’s study, six NHP models of AD, using cynomolgus monkeys, were established via ICV-A $\beta$  injection once every three days consecutively for up to 24 days.<sup>154</sup> Two of the six NHP models received daily subcutaneous injections of liraglutide beginning one week prior to ICV-A $\beta$  injection and lasted until the end of the ICV-A $\beta$  injections.<sup>154</sup> ICV-A $\beta$ -treated monkeys exhibited diffuse A $\beta$  peptides, p-Tau, tangle formation, synapse loss,

and glial activation, which recapitulated many AD features.<sup>154</sup> Reduced levels of insulin receptors were observed in the frontal cortex, hippocampus, and amygdala.<sup>154</sup> Comparing ICV-A $\beta$ -treated and ICV-A $\beta$ /liraglutide-treated monkeys, the administration of liraglutide conferred modest protection against the loss of synaptophysin, reduced density of synapses, and hyperphosphorylation of Tau in the hippocampus, frontal cortex, and amygdala.<sup>154</sup> This study illustrated the possible association between A $\beta$  and insulin dysregulation, further strengthening the theory that glucose hypometabolism and insulin receptor signalling is closely associated with AD. The protective effects of the anti-diabetes treatment, liraglutide, against AD-associated proteopathies and neuronal insulin signalling were also demonstrated, even though full protection was not achieved. Obviously, strengthening synapses and restoring neuronal insulin signalling are insufficient to treat AD, so the combination of anti-diabetic treatments and other therapeutics may be administered concurrently to modify AD progression. Another anti-diabetic drug, pioglitazone, which has an unclear biochemical mechanism of action and may be associated with mitochondria functions and oxidative stress, was also tested on male vervet monkeys to treat neurodegenerative disorders.<sup>155</sup> In the last five years, with increasing awareness of the association between diabetes and AD, the repurposing of anti-diabetic drugs for AD treatment has been launched and NHP models of AD are useful to assess their therapeutic effects prior to clinical trials involving human subjects.

Although the amyloid theory has dominated the AD field for decades, its low clinical translational rate raises concerns that AD may not be fully explained by A $\beta$ . Recent large-scale genome-wide association studies have identified over 130 susceptibility loci associated with AD risks and over half of them implicate a role for the innate immune system.<sup>148</sup> Innate immune responses are altered in both the central and peripheral pool, including microglial activation, astrocyte activation, monocyte alteration, and AD-associated pro-inflammatory profiles.<sup>148,156,157</sup> Consequently, drug repurposing of anti-inflammatory drugs has become a plausible approach to treat AD. Dimebolin (latrepirdine), a non-selective anti-histamine drug, has indicated its effectiveness in modifying dementia symptoms in the initial trials.<sup>158</sup> It was then tested on young adult (11–17 years old) and aged (20–31 years old) rhesus monkeys to evaluate its modulation of cognition.<sup>159</sup> In both young adult and aged rhesus monkeys, dimebolin increased performance on DMTS tasks, manifesting acutely improved working memory and a protracted response for at least 24 hours.<sup>159</sup> In 2015, ibuprofen, a nonsteroidal anti-inflammatory drug, was tested on five to seven conscious cynomolgus monkeys and 16 healthy subjects, and further compared the subsequent A $\beta$  burden levels after the administration of GSM-1.<sup>160</sup> A single dose of GSM-1 significantly reduced the ratio of A $\beta$ <sub>1–42</sub>:A $\beta$ <sub>1–40</sub> in plasma and CSF, but a single high dose of ibuprofen did not modulate the plasma levels of A $\beta$  in cynomolgus monkeys and human subjects.<sup>160</sup> The GSM activity of ibuprofen was not detected in this study, which is consistent with previous conclusions that only long-term administration of ibuprofen would confer moderate protection against AD.<sup>160,161</sup> As indicated by genomic studies, the development of innate immune boosters that can promote innate phagocytosis of A $\beta$  is also expected to resolve AD proteopathies.<sup>148</sup>

### Lifestyle modifications

Given the limited options of DMTs and the restricted applications of early diagnostic tools in AD, effective preventive strategies are highly encouraged to reduce an individual’s exposure to AD-associated risk factors, including dietary interventions,



physical activity, and sleeping improvement.<sup>162</sup> Calorie restriction may prevent A $\beta$  accumulation in rodent models of AD by promoting NAD<sup>+</sup>-dependent SIRT1 mediated deacetylase activity.<sup>163</sup> A 30% calorie restriction in squirrel monkeys reduced the levels of A $\beta$ <sub>1-42</sub> and A $\beta$ <sub>1-40</sub>, and the reduced portion of A $\beta$  peptides were inversely associated with SIRT1 protein in the temporal cortex of squirrel monkeys.<sup>163</sup> Most interestingly, this 30% calorie restriction elevated the activity of  $\alpha$ -secretase but did not alter that of  $\beta$ - or  $\gamma$ -secretase, as supported by decreased ROCK1 protein in the same brain region.<sup>163</sup> This study demonstrated the A $\beta$  modulating ability of calorie restriction for the first time, but the authors did not compare other AD-associated pathologies or the differences in cognitive decline between the treatment and control groups. The 30% calorie restriction also reduced stress responsiveness without affecting orientation and attention behaviour in 44 rhesus monkeys (19–31 years old).<sup>164</sup> Their stress reactivity was associated with brain atrophy in regions responsible for emotional regulation and microstructural tissue density, and this relationship was also reduced by 30% calorie restriction.<sup>164</sup> It is expected that future studies would first construct spontaneous or induced NHP models of AD and then deliver calorie restriction to specifically assess its modulation of AD-associated pathologies and behaviours. To be more specific about diet, the dietary amino acid L-serine in tofu and seaweeds slowed the development of tangles and A $\beta$  plaques in NHPs and human subjects with amyotrophic lateral sclerosis.<sup>165,166</sup> An interesting study compared Western diet, mimicking the diet consumed by American women (40–49 years old), and Mediterranean diet using middle-aged (11–13 years old) female cynomolgus monkeys.<sup>167</sup> The Western diet group presented higher grey matter volume and cortical thickness in the temporoparietal regions, which may confer protection against AD but may also be caused by neuroinflammation.<sup>167</sup> The volume of white matter was reduced in the Western diet group but remained intact in the Mediterranean group, coinciding with early biomarkers of AD neuropathology.<sup>167</sup> The observation of healthy diet and calorie restriction indicates that lifestyle modification can confer protection against AD even though their underlying mechanisms remain inconclusive, and their protective strengths remain low.

### Chinese medicine in tree shrews

In China and other East Asian countries, a wide range of traditional Chinese medical herbs have been used as therapeutic and preventative strategies for numerous disorders for thousands of years. *Panax ginseng* C.A. Mey. (ginseng) is one of the most well-known and valuable traditional medical herbs conferring anti-inflammatory, anti-tumour, and anti-oxidative effects.<sup>168</sup> Ginsenosides, the major pharmacologically active ingredient of ginseng, possess strong AChE inhibitory potential, greatly improving cognitive and memory decline in AD.<sup>168</sup> Ginsenosides play a neuroprotective role in AD by inhibiting A $\beta$  aggregation and Tau hyperphosphorylation, ameliorating inflammation, reducing apoptosis, promoting neurotrophic factors, and improving mitochondrial dysfunctions.<sup>168</sup> In 2020, a cohort of male Chinese tree shrews were administered intra-hippocampal injections of A $\beta$ <sub>25-35</sub> (A $\beta$ <sub>25-35</sub>) or control saline (CT group) to establish an induced NHP model of AD.<sup>169</sup> Six groups of the animals subsequently received intraperitoneal intragastric administration of donepezil (DN group), intraperitoneal intragastric administration of Ginsenoside Rg1 (GRg1) with low, middle, or high doses, or control saline solution (AD group) orally for eight weeks.<sup>169</sup> GRg1 oral treatment led to cognitive improvement, as assessed by Morris water maze, and decreased levels of Tau in the hippocampus and cortex in the DN and

GRg1 groups.<sup>169</sup> More specifically, tree shrews in the middle and high-GRg1 groups had significantly lower numbers of Tau<sup>+</sup> cells, compared with the low-GRg1 group and the DN group.<sup>169</sup> The subsequent 16S ribosomal RNA sequencing illustrated different profiles of gut microbiota between the different groups, in which middle and high doses of GRg1 modified the gut microbiota to resemble the CT group.<sup>169</sup> After screening for the optimal dosage of GRg1 for AD modification, another cohort of tree shrew models of AD were established via ventricle injections of A $\beta$ <sub>25-35</sub> (A $\beta$ <sub>25-35</sub>), followed by a high dose of GRg1 only.<sup>170</sup> GRg1 inhibited the expression of  $\beta$ -secretase 1 but promoted the expressions of microtubule-associated protein 2 and FOX-3 in the hippocampus of A $\beta$ <sub>25-35</sub>/GRg1-treated tree shrews compared with the A $\beta$ <sub>25-35</sub>-treated group.<sup>170</sup> A $\beta$ <sub>25-35</sub>/GRg1-treated tree shrews also demonstrated lower levels of A $\beta$ , p-Tau, and the pro-apoptotic factor Bax and increased levels of BCL-2 in the hippocampus and cortex, compared with the A $\beta$ <sub>25-35</sub>-treated group.<sup>170</sup> More recently, GRg1 was shown to increase the antioxidant activities of SOD, CAT, GPx and reduce the inflammatory factors interleukin-1 and IBA-1.<sup>171</sup> The ratio of BCL-2 to Bax was increased in the A $\beta$ <sub>25-35</sub>/GRg1-treated group, accompanied by reduced expression of Caspase-3, GSK-3 $\beta$ , and  $\beta$ -catenin.<sup>171</sup> In brief, high doses of GRg1 are promising at alleviating oxidative stresses, pro-inflammatory markers, pro-apoptotic activities, AD-associated proteopathies, and cognitive deficits induced by A $\beta$ <sub>25-35</sub> injections in tree shrews.<sup>170,171</sup> GRg1 oral treatment is also closely associated with gut microbiota AD by altering the abundances of *Bacteroidetes*, *Proteobacteria*, *Verrucomicrobia*, and *Lactobacillaceae*.<sup>169,170</sup> These studies utilized appropriate study design, comprehensive histological assessment, and cognitive examination, forming a theoretical basis for the examination of GRg1 in clinical trials involving human subjects.

### Future directions

It is anticipated that the NHP model of AD will be used in more and more AD drug development projects, to evaluate the drug administration routes, pharmacokinetics, pharmacodynamics, tolerability, safety, and most importantly, the drug efficacy prior to Phase I clinical trials. Thus, great effort is needed to improve the current NHP models of AD, particularly in imaging, laboratory biomarkers and behavioral tests for drug efficacy evaluation. A $\beta$  PET scan with appropriate radioisotope labeled tracers will be applied in the next couple of years, together with novel blood and urine biomarkers. These studies will therefore provide necessary data and solid evidence to facilitate clinical trials in human subjects.

### Conclusions

After the first identification of AD over 100 years ago, the field is still attempting to understand the fundamental aetiology and pathogenesis underlying AD. The application of animal models of AD that fully recapitulate AD-associated pathologies and symptoms can greatly advance our understanding of the molecular, cellular, physiological, and psychological processes along the course of the disease. This review has summarised the spontaneous and induced NHP models of AD and their recent contributions to AD research. Spontaneous NHP models of AD exhibit wide-spread A $\beta$  depositions, CAA, glial activation, and moderate cognitive decline at the elderly age, while NHP models of AD induced by ICV-A $\beta$ <sub>25-35</sub>, brain homogenates, FA, and ICV-STZ further present with AD-resembling p-Tau, minor NFTs, and brain atrophy. The co-occurrence of all AD-associated pathologies and behavioural changes is

rarely observed in rodent models, but it is reported in several NHP studies due to the close phylogenetic relationship, similar AD-associated genetics, similar neuroanatomy, physiology, neuronal functions, and high-order cognitive, emotional, and social behaviours between NHPs and human subjects. In the last two decades, NHP models of AD are increasingly involved in the development of novel PET tracers, A $\beta$  vaccines, DMTs, and dietary modifications to aid in their translation into clinical trials involving human subjects, aiming at improving the diagnostic criteria, preventative strategies, and therapeutic treatments for AD. However, the investigations into the NHP models of AD are associated with some limitations. Compared with rodent models of AD, the use of NHP models of AD requires higher financial costs, greater genetic manipulation, smaller sample sizes, and more specialised researchers and facilities. There is still an absence of a standardised protocol to establish a broadly accepted NHP model of AD, which may increase the discrepancies across different studies. Based on the studies by Yue and Forný-Germano, the field should generate a guideline which recommends that certain inducers, dosages of inducers, injection frequencies, and inoculation periods should be met to produce reliable NHP models of AD. A good study design that assesses a broad range of AD-associated pathologies and behaviour changes must be incorporated into NHP studies to enable peer researchers to comprehensively interpretate the effects of PET tracers, A $\beta$  vaccines, DMTs, or lifestyle modifications. The establishment of a standardised NHP model of AD and the engagement of a comprehensive assessment of NHPs will greatly accelerate the translation from NHP discoveries into clinical trials involving human subjects, thus greatly speeding up the discoveries of biomarkers and DMTs for AD.

### Acknowledgments

The authors are grateful to the University of Melbourne for providing open access to PubMed for literature review.

### Funding

This work was supported by the Melbourne Research Scholarship provided by the Florey Institute of Neuroscience and Mental Health, the University of Melbourne, and Qiankang Life Science Melbourne R&D Centre. We sincerely appreciate funding support from the Ministry of Science and Technology of China (program grant No. SQ2018YFC200022 to BG), and the Victorian Government's Operational Infrastructure Support Grant to the Florey Institute.

### Conflict of interest

Ben J. Gu has been an Editor-in-Chief of the *Journal of Exploratory Research in Pharmacology* since June 2021. The authors have no other conflicts of interests to declare.

### Author contributions

Study design (YL and BG), writing (YL and BG), critical revision of the manuscript (YL), supervision (BG).

### References

- [1] Scheltens P, De Strooper B, Kivipelto M, Holstege H, Ch  telat G, Teunissen CE, *et al*. Alzheimer's disease. *Lancet* 2021;397(10284):1577–1590. doi:10.1016/S0140-6736(20)32205-4, PMID:33667416.
- [2] Van Dam D, De Deyn PP. Non human primate models for Alzheimer's disease-related research and drug discovery. *Expert Opin Drug Discov* 2017;12(2):187–200. doi:10.1080/17460441.2017.1271320, PMID:27960560.
- [3] DeTure MA, Dickson DW. The neuropathological diagnosis of Alzheimer's disease. *Mol Neurodegener* 2019;14(1):32. doi:10.1186/s13024-019-0333-5, PMID:31375134.
- [4] De Strooper B, Karran E. The Cellular Phase of Alzheimer's Disease. *Cell* 2016;164(4):603–615. doi:10.1016/j.cell.2015.12.056, PMID:26871627.
- [5] Sperling RA, Aisen PS, Beckett LA, Bennett DA, Craft S, Fagan AM, *et al*. Toward defining the preclinical stages of Alzheimer's disease: recommendations from the National Institute on Aging-Alzheimer's Association workgroups on diagnostic guidelines for Alzheimer's disease. *Alzheimers Dement* 2011;7(3):280–292. doi:10.1016/j.jalz.2011.03.003, PMID:21514248.
- [6] McKhann GM, Knopman DS, Chertkow H, Hyman BT, Jack CR Jr, Kawas CH, *et al*. The diagnosis of dementia due to Alzheimer's disease: recommendations from the National Institute on Aging-Alzheimer's Association workgroups on diagnostic guidelines for Alzheimer's disease. *Alzheimers Dement* 2011;7(3):263–269. doi:10.1016/j.jalz.2011.03.005, PMID:21514250.
- [7] Selkoe DJ, Hardy J. The amyloid hypothesis of Alzheimer's disease at 25 years. *EMBO Mol Med* 2016;8(6):595–608. doi:10.15252/emmm.201606210, PMID:27025652.
- [8] Thal DR, R  b U, Orantes M, Braak H. Phases of A beta-deposition in the human brain and its relevance for the development of AD. *Neurology* 2002;58(12):1791–1800. doi:10.1212/wnl.58.12.1791, PMID:12084879.
- [9] Greenberg SM, Bacskai BJ, Hernandez-Guillamon M, Pruzin J, Sperling R, van Veluw SJ. Cerebral amyloid angiopathy and Alzheimer disease - one peptide, two pathways. *Nat Rev Neurol* 2020;16(1):30–42. doi:10.1038/s41582-019-0281-2, PMID:31827267.
- [10] Chang CW, Shao E, Mucke L. Tau: Enabler of diverse brain disorders and target of rapidly evolving therapeutic strategies. *Science* 2021;371:6532. doi:10.1126/science.abb8255, PMID:33632820.
- [11] Medeiros R, Baglietto-Vargas D, LaFerla FM. The role of tau in Alzheimer's disease and related disorders. *CNS Neurosci Ther* 2011;17(5):514–524. doi:10.1111/j.1755-5949.2010.00177.x, PMID:20553310.
- [12] Braak H, Alafuzoff I, Arzberger T, Kretschmar H, Del Tredici K. Staging of Alzheimer disease-associated neurofibrillary pathology using paraffin sections and immunocytochemistry. *Acta Neuropathol* 2006;112(4):389–404. doi:10.1007/s00401-006-0127-z, PMID:16906426.
- [13] Cacace R, Slegers K, Van Broeckhoven C. Molecular genetics of early-onset Alzheimer's disease revisited. *Alzheimers Dement* 2016;12(6):733–748. doi:10.1016/j.jalz.2016.01.012, PMID:27016693.
- [14] Thinakaran G, Koo EH. Amyloid precursor protein trafficking, processing, and function. *J Biol Chem* 2008;283(44):29615–29619. doi:10.1074/jbc.R800019200, PMID:18650430.
- [15] Poirier J, Davignon J, Bouthillier D, Kogan S, Bertrand P, Gauthier S. Apolipoprotein E polymorphism and Alzheimer's disease. *Lancet* 1993;342(8873):697–699. doi:10.1016/0140-6736(93)91705-q, PMID:8103819.
- [16] Neuner SM, Tcw J, Goate AM. Genetic architecture of Alzheimer's disease. *Neurobiol Dis* 2020;143:104976. doi:10.1016/j.nbd.2020.104976, PMID:32565066.
- [17] Sanchez-Varo R, Mejias-Ortega M, Fernandez-Valenzuela JJ, Nu  ez-Diaz C, Caceres-Palomo L, Vegas-Gomez L, *et al*. Transgenic Mouse Models of Alzheimer's Disease: An Integrative Analysis. *Int J Mol Sci* 2022;23(10):5404. doi:10.3390/ijms23105404, PMID:35628216.
- [18] Moss MB, Moore TL, Schettler SP, Killiany R, Rosene D. Successful vs. Unsuccessful Aging in the Rhesus Monkey. In: Riddle DR (ed). *Brain Aging: Models, Methods, and Mechanisms*. Boca Raton (FL): CRC Press/Taylor & Francis; 2007. Chapter 2. Available from: <https://www.ncbi.nlm.nih.gov/books/NBK1833/>.
- [19] Heuer E, Rosen RF, Cintron A, Walker LC. Nonhuman primate models of Alzheimer-like cerebral proteopathy. *Curr Pharm Des* 2012;18(8):1159–1169. doi:10.2174/138161212799315885, PMID:

- 22288403.
- [20] Li HW, Zhang L, Qin C. Current state of research on non-human primate models of Alzheimer's disease. *Animal Model Exp Med* 2019;2(4):227–238. doi:10.1002/ame2.12092, PMID:31942555.
- [21] Bartus RT, Fleming D, Johnson HR. Aging in the rhesus monkey: debilitating effects on short-term memory. *J Gerontol* 1978;33(6):858–871. doi:10.1093/geronj/33.6.858, PMID:106081.
- [22] Cowan N. What are the differences between long-term, short-term, and working memory? *Prog Brain Res* 2008;169:323–338. doi:10.1016/s0079-6123(07)00020-9, PMID:18394484.
- [23] Bartus RT, Dean RL 3rd, Fleming DL. Aging in the rhesus monkey: effects on visual discrimination learning and reversal learning. *J Gerontol* 1979;34(2):209–219. doi:10.1093/geronj/34.2.209, PMID:108323.
- [24] Wenk GL. A primate model of Alzheimer's disease. *Behav Brain Res* 1993;57(2):117–122. doi:10.1016/0166-4328(93)90127-c, PMID:8117419.
- [25] Dudkin KN, Chueva IV, Makarov FN, Beach TG, Roher A. Impaired processes of working memory in the monkey model of Alzheimer's disease. *Dokl Biol Sci* 2002;383:106–108. doi:10.1023/a:1015373420424, PMID:12053557.
- [26] Dudkin KN, Chueva IV, Makarov FN, Bich TG, Roher AE. Impairments in working memory and decision-taking processes in monkeys in a model of Alzheimer's disease. *Neurosci Behav Physiol* 2005;35(3):281–289. doi:10.1007/s11055-005-0057-6, PMID:15875490.
- [27] Dudkin KN, Chueva IV, Makarov FN, Bich TG, Roher AE. Disorders of learning and memory processes in a monkey model of Alzheimer's disease: the role of the associative area of the cerebral cortex. *Neurosci Behav Physiol* 2006;36(8):789–799. doi:10.1007/s11055-006-0089-6, PMID:16964455.
- [28] Presty SK, Bachevalier J, Walker LC, Struble RG, Price DL, Mishkin M, *et al.* Age differences in recognition memory of the rhesus monkey (*Macaca mulatta*). *Neurobiol Aging* 1987;8(5):435–440. doi:10.1016/0197-4580(87)90038-8, PMID:3683724.
- [29] Rapp PR, Amaral DG. Evidence for task-dependent memory dysfunction in the aged monkey. *J Neurosci* 1989;9(10):3568–3576. doi:10.1523/JNEUROSCI.09-10-03568.1989, PMID:2795141.
- [30] Bachevalier J. Behavioral changes in aged rhesus monkeys. *Neurobiol Aging* 1993;14(6):619–621. doi:10.1016/0197-4580(93)90048-g, PMID:8295665.
- [31] Moss MB, Killiany RJ, Lai ZC, Rosene DL, Herndon JG. Recognition memory span in rhesus monkeys of advanced age. *Neurobiol Aging* 1997;18(1):13–19. doi:10.1016/s0197-4580(96)00211-4, PMID:8983028.
- [32] Calhoun ME, Mao Y, Roberts JA, Rapp PR. Reduction in hippocampal cholinergic innervation is unrelated to recognition memory impairment in aged rhesus monkeys. *J Comp Neurol* 2004;475(2):238–246. doi:10.1002/cne.20181, PMID:15211464.
- [33] Struble RG, Price DL Jr, Cork LC, Price DL. Senile plaques in cortex of aged normal monkeys. *Brain Res* 1985;361(1-2):267–275. doi:10.1016/0006-8993(85)91298-3, PMID:4084799.
- [34] Selkoe DJ, Bell DS, Podlisny MB, Price DL, Cork LC. Conservation of brain amyloid proteins in aged mammals and humans with Alzheimer's disease. *Science* 1987;235(4791):873–877. doi:10.1126/science.3544219, PMID:3544219.
- [35] Walker LC, Kitt CA, Schwam E, Buckwald B, Garcia F, Sepinwall J, *et al.* Senile plaques in aged squirrel monkeys. *Neurobiol Aging* 1987;8(4):291–296. doi:10.1016/0197-4580(87)90067-4, PMID:3306432.
- [36] Cork LC, Masters C, Beyreuther K, Price DL. Development of senile plaques. Relationships of neuronal abnormalities and amyloid deposits. *Am J Pathol* 1990;137(6):1383–1392. PMID:1701963.
- [37] Heilbroner PL, Kemper TL. The cytoarchitectonic distribution of senile plaques in three aged monkeys. *Acta Neuropathol* 1990;81(1):60–65. doi:10.1007/bf00662638, PMID:1707575.
- [38] Thal DR, Capetillo-Zarate E, Del Tredici K, Braak H. The development of amyloid beta protein deposits in the aged brain. *Sci Aging Knowledge Environ* 2006;2006(6):re1. doi:10.1126/sageke.2006.6.re1, PMID:16525193.
- [39] Podlisny MB, Tolan DR, Selkoe DJ. Homology of the amyloid beta protein precursor in monkey and human supports a primate model for beta amyloidosis in Alzheimer's disease. *Am J Pathol* 1991;138(6):1423–1435. PMID:1905108.
- [40] Nakamura S, Kiatipattanasakul W, Nakayama H, Ono F, Sakakibara I, Yoshikawa Y, *et al.* Immunohistochemical characteristics of the constituents of senile plaques and amyloid angiopathy in aged cynomolgus monkeys. *J Med Primatol* 1996;25(4):294–300. doi:10.1111/j.1600-0684.1996.tb00213.x, PMID:8906609.
- [41] Gearing M, Tigges J, Mori H, Mirra SS. A beta40 is a major form of beta-amyloid in nonhuman primates. *Neurobiol Aging* 1996;17(6):903–908. doi:10.1016/s0197-4580(96)00164-9, PMID:9363802.
- [42] Kanemaru K, Iwatsubo T, Ihara Y. Comparable amyloid beta-protein (A beta) 42(43) and A beta 40 deposition in the aged monkey brain. *Neurosci Lett* 1996;214(2-3):196–198. doi:10.1016/0304-3940(96)12893-7, PMID:8878117.
- [43] Bons N, Mestre N, Petter A. Senile plaques and neurofibrillary changes in the brain of an aged lemurian primate, *Microcebus murinus*. *Neurobiol Aging* 1992;13(1):99–105. doi:10.1016/0197-4580(92)90016-q, PMID:1542387.
- [44] Bons N, Mestre N, Ritchie K, Petter A, Podlisny M, Selkoe D. Identification of amyloid beta protein in the brain of the small, short-lived lemurian primate *Microcebus murinus*. *Neurobiol Aging* 1994;15(2):215–220. doi:10.1016/0197-4580(94)90115-5, PMID:7838294.
- [45] Uno H, Alsum PB, Dong S, Richardson R, Zimbric ML, Thieme CS, *et al.* Cerebral amyloid angiopathy and plaques, and visceral amyloidosis in aged macaques. *Neurobiol Aging* 1996;17(2):275–281. doi:10.1016/0197-4580(95)02063-2, PMID:8744409.
- [46] Bons N, Rieger F, Prudhomme D, Fisher A, Krause KH. *Microcebus murinus*: a useful primate model for human cerebral aging and Alzheimer's disease? *Genes Brain Behav* 2006;5(2):120–130. doi:10.1111/j.1601-183X.2005.00149.x, PMID:16507003.
- [47] Oikawa N, Kimura N, Yanagisawa K. Alzheimer-type tau pathology in advanced aged nonhuman primate brains harboring substantial amyloid deposition. *Brain Res* 2010;1315:137–149. doi:10.1016/j.brainres.2009.12.005, PMID:20004650.
- [48] Norvin D, Kim G, Baker-Nigh A, Geula C. Accumulation and age-related elevation of amyloid- $\beta$  within basal forebrain cholinergic neurons in the rhesus monkey. *Neuroscience* 2015;298:102–111. doi:10.1016/j.neuroscience.2015.04.011S0306-4522(15)00342-5, PMID:25869619.
- [49] Paspalas CD, Carlyle BC, Leslie S, Preuss TM, Crimins JL, Huttner AJ, *et al.* The aged rhesus macaque manifests Braak stage III/IV Alzheimer's-like pathology. *Alzheimers Dement* 2018;14(5):680–691. doi:10.1016/j.jalz.2017.11.005, PMID:29241829.
- [50] Koinuma S, Shimozawa N, Yasutomi Y, Kimura N. Aging induces abnormal accumulation of A $\beta$  in extracellular vesicle and/or intraluminal membrane vesicle-rich fractions in nonhuman primate brain. *Neurobiol Aging* 2021;106:268–281. doi:10.1016/j.neurobiolaging.2021.06.022, PMID:34329965.
- [51] Schmidtke D, Zimmermann E, Trouche SG, Fontès P, Verdier JM, Mestre-Francés N. Linking cognition to age and amyloid- $\beta$  burden in the brain of a nonhuman primate (*Microcebus murinus*). *Neurobiol Aging* 2020;94:207–216. doi:10.1016/j.neurobiolaging.2020.03.025, PMID:32650184.
- [52] Uchihara T, Endo K, Kondo H, Okabayashi S, Shimozawa N, Yasutomi Y, *et al.* Tau pathology in aged cynomolgus monkeys is progressive supranuclear palsy/corticobasal degeneration- but not Alzheimer disease-like -Ultrastructural mapping of tau by EDX. *Acta Neuropathol Commun* 2016;4(1):118. doi:10.1186/s40478-016-0385-5, PMID:27842611.
- [53] Pawlik M, Fuchs E, Walker LC, Levy E. Primate-like amyloid-beta sequence but no cerebral amyloidosis in aged tree shrews. *Neurobiol Aging* 1999;20(1):47–51. doi:10.1016/s0197-4580(99)00017-2, PMID:10466892.
- [54] Yamashita A, Fuchs E, Taira M, Hayashi M. Amyloid beta (A $\beta$ ) protein- and amyloid precursor protein (APP)-immunoreactive structures in the brains of aged tree shrews. *Curr Aging Sci* 2010;3(3):230–238. doi:10.2174/1874609811003030230, PMID:20735344.
- [55] Walker LC, Masters C, Beyreuther K, Price DL. Amyloid in the brains of aged squirrel monkeys. *Acta Neuropathol* 1990;80(4):381–387. doi:10.1007/bf00307691, PMID:2239150.

- [56] Elfenbein HA, Rosen RF, Stephens SL, Switzer RC, Smith Y, Pare J, *et al*. Cerebral beta-amyloid angiopathy in aged squirrel monkeys. *Histol Histopathol* 2007;22(2):155–167. doi:10.14670/hh-22.155, PMID:17149688.
- [57] Mestre-Francés N, Keller E, Calenda A, Barelli H, Checler F, Bons N. Immunohistochemical analysis of cerebral cortical and vascular lesions in the primate *Microcebus murinus* reveal distinct amyloid beta1-42 and beta1-40 immunoreactivity profiles. *Neurobiol Dis* 2000;7(1):1–8. doi:10.1006/nbdi.1999.0270, PMID:10671318.
- [58] Silhol S, Calenda A, Jallageas V, Mestre-Frances N, Bellis M, Bons N. beta-Amyloid protein precursor in *Microcebus murinus*: genotyping and brain localization. *Neurobiol Dis* 1996;3(3):169–182. doi:10.1006/nbdi.1996.0017, PMID:8980017.
- [59] Martin LJ, Sisodia SS, Koo EH, Cork LC, Dellovade TL, Weidemann A, *et al*. Amyloid precursor protein in aged nonhuman primates. *Proc Natl Acad Sci U S A* 1991;88(4):1461–1465. doi:10.1073/pnas.88.4.1461, PMID:1899927.
- [60] Fukumoto H, Rosene DL, Moss MB, Raju S, Hyman BT, Irizarry MC. Beta-secretase activity increases with aging in human, monkey, and mouse brain. *Am J Pathol* 2004;164(2):719–725. doi:10.1016/s0002-9440(10)63159-8, PMID:14742275.
- [61] Fan Y, Luo R, Su LY, Xiang Q, Yu D, Xu L, *et al*. Does the Genetic Feature of the Chinese Tree Shrew (*Tupaia belangeri chinensis*) Support Its Potential as a Viable Model for Alzheimer's Disease Research? *J Alzheimers Dis* 2018;61(3):1015–1028. doi:10.3233/jad-170594, PMID:29332044.
- [62] Fan Y, Ye MS, Zhang JY, Xu L, Yu DD, Gu TL, *et al*. Chromosomal level assembly and population sequencing of the Chinese tree shrew genome. *Zool Res* 2019;40(6):506–521. doi:10.24272/j.issn.2095-8137.2019.063, PMID:31418539.
- [63] Calenda A, Mestre-Francés N, Czech C, Pradier L, Petter A, Bons N, *et al*. Molecular cloning, sequencing, and brain expression of the presenilin 1 gene in *Microcebus murinus*. *Biochem Biophys Res Commun* 1996;228(2):430–439. doi:10.1006/bbrc.1996.1678, PMID:8920931.
- [64] Calenda A, Mestre-Francés N, Czech C, Pradier L, Petter A, Perret M, *et al*. Cloning of the presenilin 2 cDNA and its distribution in brain of the primate, *Microcebus murinus*: coexpression with betaAPP and Tau proteins. *Neurobiol Dis* 1998;5(5):323–333. doi:10.1006/nbdi.1998.0205, PMID:10069575.
- [65] Kimura N, Nakamura SI, Honda T, Takashima A, Nakayama H, Ono F, *et al*. Age-related changes in the localization of presenilin-1 in cynomolgus monkey brain. *Brain Res* 2001;922(1):30–41. doi:10.1016/s0006-8993(01)03146-8, PMID:11730699.
- [66] Kimura N, Nakamura SI, Ono F, Sakakibara I, Ishii Y, Kyuwa S, *et al*. Presenilin-2 in the cynomolgus monkey brain: investigation of age-related changes. *Primates* 2004;45(3):167–175. doi:10.1007/s10329-004-0076-x, PMID:14986149.
- [67] Li MX, Wang WG, Kuang DX, Ruan LY, Li XH, Huang X, *et al*. Identification, characterization and expression profiles of PSEN2 in the Chinese tree shrew (*Tupaia belangeri chinensis*). *J Integr Neurosci* 2020;19(2):249–257. doi:10.31083/j.jin.2020.02.28, PMID:32706189.
- [68] Calenda A, Jallageas V, Silhol S, Bellis M, Bons N. Identification of a unique apolipoprotein E allele in *Microcebus murinus*; ApoE brain distribution and co-localization with beta-amyloid and tau proteins. *Neurobiol Dis* 1995;2(3):169–176. doi:10.1006/nbdi.1995.0018, PMID:9174000.
- [69] Fainman J, Eid MD, Ervin FR, Palmour RM. A primate model for Alzheimer's disease: investigation of the apolipoprotein E profile of the vervet monkey of St. Kitts. *Am J Med Genet B Neuropsychiatr Genet* 2007;144B(6):818–819. doi:10.1002/ajmg.b.30276, PMID:17373728.
- [70] Gearing M, Rebeck GW, Hyman BT, Tigges J, Mirra SS. Neuropathology and apolipoprotein E profile of aged chimpanzees: implications for Alzheimer disease. *Proc Natl Acad Sci U S A* 1994;91(20):9382–9386. doi:10.1073/pnas.91.20.9382, PMID:7937774.
- [71] Härtig W, Klein C, Brauer K, Schüppel KF, Arendt T, Brückner G, *et al*. Abnormally phosphorylated protein tau in the cortex of aged individuals of various mammalian orders. *Acta Neuropathol* 2000;100(3):305–312. doi:10.1007/s004010000183, PMID:10965801.
- [72] Datta D, Leslie SN, Wang M, Morozov YM, Yang S, Mentone S, *et al*. Age-related calcium dysregulation linked with tau pathology and impaired cognition in non-human primates. *Alzheimers Dement* 2021;17(6):920–932. doi:10.1002/alz.12325, PMID:33829643.
- [73] Bons N, Jallageas V, Silhol S, Mestre-Frances N, Petter A, Delacourte A. Immunocytochemical characterization of Tau proteins during cerebral aging of the lemurian primate *Microcebus murinus*. *C R Acad Sci III* 1995;318(1):77–83. PMID:7757807.
- [74] Giannakopoulos P, Silhol S, Jallageas V, Mallet J, Bons N, Bouras C, *et al*. Quantitative analysis of tau protein-immunoreactive accumulations and beta amyloid protein deposits in the cerebral cortex of the mouse lemur, *Microcebus murinus*. *Acta Neuropathol* 1997;94(2):131–139. doi:10.1007/s004010050684, PMID:9255387.
- [75] Latimer CS, Shively CA, Keene CD, Jorgensen MJ, Andrews RN, Register TC, *et al*. A nonhuman primate model of early Alzheimer's disease pathologic change: Implications for disease pathogenesis. *Alzheimers Dement* 2019;15(1):93–105. doi:10.1016/j.jalz.2018.06.3057, PMID:30467082.
- [76] Rodriguez-Callejas JD, Fuchs E, Perez-Cruz C. Evidence of Tau Hyperphosphorylation and Dystrophic Microglia in the Common Marmoset. *Front Aging Neurosci* 2016;8:315. doi:10.3389/fnagi.2016.00315, PMID:28066237.
- [77] Rodriguez-Callejas JD, Fuchs E, Perez-Cruz C. Increased oxidative stress, hyperphosphorylation of tau, and dystrophic microglia in the hippocampus of aged *Tupaia belangeri*. *Glia* 2020;68(9):1775–1793. doi:10.1002/glia.23804, PMID:32096580.
- [78] Gazzaley AH, Thakker MM, Hof PR, Morrison JH. Preserved number of entorhinal cortex layer II neurons in aged macaque monkeys. *Neurobiol Aging* 1997;18(5):549–553. doi:10.1016/s0197-4580(97)00112-7, PMID:9390783.
- [79] Keuker JI, Luiten PG, Fuchs E. Preservation of hippocampal neuron numbers in aged rhesus monkeys. *Neurobiol Aging* 2003;24(1):157–165. doi:10.1016/s0197-4580(02)00062-3, PMID:12493561.
- [80] Edler MK, Munger EL, Meindl RS, Hopkins WD, Ely JJ, Erwin JM, *et al*. Neuron loss associated with age but not Alzheimer's disease pathology in the chimpanzee brain. *Philos Trans R Soc Lond B Biol Sci* 2020;375(1811):20190619. doi:10.1098/rstb.2019.0619, PMID:32951541.
- [81] Frye BM, Craft S, Register TC, Kim J, Whitlow CT, Barcus RA, *et al*. Early Alzheimer's disease-like reductions in gray matter and cognitive function with aging in nonhuman primates. *Alzheimers Dement (N Y)* 2022;8(1):e12284. doi:10.1002/trc2.12284, PMID:35310523.
- [82] Podlisy MB, Stephenson DT, Frosch MP, Tolan DR, Lieberburg I, Clemens JA, *et al*. Microinjection of synthetic amyloid beta-protein in monkey cerebral cortex fails to produce acute neurotoxicity. *Am J Pathol* 1993;142(1):17–24. PMID:8424453.
- [83] McKee AC, Kowall NW, Schumacher JS, Beal MF. The neurotoxicity of amyloid beta protein in aged primates. *Amyloid* 1998;5(1):1–9. doi:10.3109/13506129809007283, PMID:9546999.
- [84] Geula C, Wu CK, Saroff D, Lorenzo A, Yuan M, Yankner BA. Aging renders the brain vulnerable to amyloid beta-protein neurotoxicity. *Nat Med* 1998;4(7):827–831. doi:10.1038/nm0798-827, PMID:9662375.
- [85] Li W, Wu Y, Min F, Li Z, Huang J, Huang R. A nonhuman primate model of Alzheimer's disease generated by intracranial injection of amyloid- $\beta$ 42 and thiorphan. *Metab Brain Dis* 2010;25(3):277–284. doi:10.1007/s11011-010-9207-9, PMID:20838863.
- [86] Beckman D, Ott S, Donis-Cox K, Janssen WG, Bliss-Moreau E, Rudebeck PH, *et al*. Oligomeric A $\beta$  in the monkey brain impacts synaptic integrity and induces accelerated cortical aging. *Proc Natl Acad Sci U S A* 2019;116(52):26239–26246. doi:10.1073/pnas.1902301116, PMID:31871145.
- [87] Beckman D, Morrison JH. Towards developing a rhesus monkey model of early Alzheimer's disease focusing on women's health. *Am J Primatol* 2021;83(11):e23289. doi:10.1002/ajp.23289, PMID:34056733.
- [88] Forny-Germano L, Lyra E Silva NM, Batista AF, Brito-Moreira J, Gralle M, Boehnke SE, *et al*. Alzheimer's disease-like pathology induced by amyloid- $\beta$  oligomers in nonhuman primates. *J Neurosci* 2014;34(41):13629–13643. doi:10.1523/JNEUROSCI.1353-14.2014, PMID:25297091.
- [89] Jebelli JD, Piers TM. Amyloid- $\beta$  oligomers unveil a novel primate model of sporadic Alzheimer's disease. *Front Neurosci* 2015;9:47. doi:10.3389/fnins.2015.00047, PMID:25852450.

- [90] Yue F, Feng S, Lu C, Zhang T, Tao G, Liu J, *et al.* Synthetic amyloid- $\beta$  oligomers drive early pathological progression of Alzheimer's disease in nonhuman primates. *iScience* 2021;24(10):103207. doi:10.1016/j.isci.2021.103207, PMID:34704001.
- [91] Wakeman DR, Weed MR, Perez SE, Cline EN, Viola KL, Wilcox KC, *et al.* Intrathecal amyloid-beta oligomer administration increases tau phosphorylation in the medial temporal lobe in the African green monkey: A nonhuman primate model of Alzheimer's disease. *Neuropathol Appl Neurobiol* 2022;48(4):e12800. doi:10.1111/nan.12800, PMID:35156715.
- [92] Lin N, Xiong LL, Zhang RP, Zheng H, Wang L, Qian ZY, *et al.* Injection of A $\beta$ 1-40 into hippocampus induced cognitive lesion associated with neuronal apoptosis and multiple gene expressions in the tree shrew. *Apoptosis* 2016;21(5):621–640. doi:10.1007/s10495-016-1227-4, PMID:26897171.
- [93] Baker HF, Ridley RM, Duchon LW, Crow TJ, Bruton CJ. Induction of beta (A4)-amyloid in primates by injection of Alzheimer's disease brain homogenate. Comparison with transmission of spongiform encephalopathy. *Mol Neurobiol* 1994;8(1):25–39. doi:10.1007/bf02778005, PMID:8086126.
- [94] Maclean CJ, Baker HF, Ridley RM, Mori H. Naturally occurring and experimentally induced beta-amyloid deposits in the brains of marmosets (*Callithrix jacchus*). *J Neural Transm (Vienna)* 2000;107(7):799–814. doi:10.1007/s007020070060, PMID:11005545.
- [95] Ridley RM, Baker HF, Windle CP, Cummings RM. Very long term studies of the seeding of beta-amyloidosis in primates. *J Neural Transm (Vienna)* 2006;113(9):1243–1251. doi:10.1007/s00702-005-0385-2, PMID:16362635.
- [96] Lam S, Petit F, Hérard AS, Boluda S, Eddarkaoui S, Guillermier M, *et al.* E. B. Neuropathology Network. Transmission of amyloid-beta and tau pathologies is associated with cognitive impairments in a primate. *Acta Neuropathol Commun* 2021;9(1):165. doi:10.1186/s40478-021-01266-8, PMID:34641980.
- [97] Kamat PK. Streptozotocin induced Alzheimer's disease like changes and the underlying neural degeneration and regeneration mechanism. *Neural Regen Res* 2015;10(7):1050–1052. doi:10.4103/1673-5374.160076, PMID:26330820.
- [98] Heo JH, Lee SR, Lee ST, Lee KM, Oh JH, Jang DP, *et al.* Spatial distribution of glucose hypometabolism induced by intracerebroventricular streptozotocin in monkeys. *J Alzheimers Dis* 2011;25(3):517–523. doi:10.3233/JAD-2011-102079, PMID:21471644.
- [99] Lee Y, Kim YH, Park SJ, Huh JW, Kim SH, Kim SU, *et al.* Insulin/IGF signaling-related gene expression in the brain of a sporadic Alzheimer's disease monkey model induced by intracerebroventricular injection of streptozotocin. *J Alzheimers Dis* 2014;38(2):251–267. doi:10.3233/JAD-130776, PMID:23948941.
- [100] Park SJ, Kim YH, Nam GH, Choe SH, Lee SR, Kim SU, *et al.* Quantitative expression analysis of APP pathway and tau phosphorylation-related genes in the ICV STZ-induced non-human primate model of sporadic Alzheimer's disease. *Int J Mol Sci* 2015;16(2):2386–2402. doi:10.3390/ijms16022386, PMID:25622254.
- [101] Yeo HG, Lee Y, Jeon CY, Jeong KJ, Jin YB, Kang P, *et al.* Characterization of Cerebral Damage in a Monkey Model of Alzheimer's Disease Induced by Intracerebroventricular Injection of Streptozotocin. *J Alzheimers Dis* 2015;46(4):989–1005. doi:10.3233/JAD-143222, PMID:25881906.
- [102] Wu J, Basha MR, Brock B, Cox DP, Cardozo-Pelaez F, McPherson CA, *et al.* Alzheimer's disease (AD)-like pathology in aged monkeys after infantile exposure to environmental metal lead (Pb): evidence for a developmental origin and environmental link for AD. *J Neurosci* 2008;28(1):3–9. doi:10.1523/JNEUROSCI.4405-07.200828/1/3, PMID:18171917.
- [103] Wang F, Chen D, Wu P, Klein C, Jin C. Formaldehyde, Epigenetics, and Alzheimer's Disease. *Chem Res Toxicol* 2019;32(5):820–830. doi:10.1021/acs.chemrestox.9b00090, PMID:30964647.
- [104] Yang M, Miao J, Rizak J, Zhai R, Wang Z, Huma T, *et al.* Alzheimer's disease and methanol toxicity (part 2): lessons from four rhesus macaques (*Macaca mulatta*) chronically fed methanol. *J Alzheimers Dis* 2014;41(4):1131–1147. doi:10.3233/JAD-131532, PMID:24787917.
- [105] Zhai R, Rizak J, Zheng N, He X, Li Z, Yin Y, *et al.* Alzheimer's Disease-Like Pathologies and Cognitive Impairments Induced by Formaldehyde in Non-Human Primates. *Curr Alzheimer Res* 2018;15(14):1304–1321. doi:10.2174/1567205015666180904150118, PMID:30182853.
- [106] Rosen RF, Walker LC, Levine H 3rd. PIB binding in aged primate brain: enrichment of high-affinity sites in humans with Alzheimer's disease. *Neurobiol Aging* 2011;32(2):223–234. doi:10.1016/j.neurobiolaging.2009.02.01150197-4580(09)00046-3, PMID:19329226.
- [107] Hostetler ED, Sanabria-Bohórquez S, Fan H, Zeng Z, Gammage L, Miller P, *et al.* [18F]Fluoroazabenzoxazoles as potential amyloid plaque PET tracers: synthesis and in vivo evaluation in rhesus monkey. *Nucl Med Biol* 2011;38(8):1193–1203. doi:10.1016/j.nucmedbio.2011.04.004, PMID:21741254.
- [108] Hillmer AT, Li S, Zheng MQ, Scheunemann M, Lin SF, Nabulsi N, *et al.* PET imaging of  $\alpha(7)$  nicotinic acetylcholine receptors: a comparative study of [(18)F]ASEM and [(18)F]DBT-10 in nonhuman primates, and further evaluation of [(18)F]ASEM in humans. *Eur J Nucl Med Mol Imaging* 2017;44(6):1042–1050. doi:10.1007/s00259-017-3621-8, PMID:28120003.
- [109] Gary C, Lam S, Hérard AS, Koch JE, Petit F, Gipchtein P, *et al.* Encephalopathy induced by Alzheimer brain inoculation in a non-human primate. *Acta Neuropathol Commun* 2019;7(1):126. doi:10.1186/s40478-019-0771-x, PMID:31481130.
- [110] Heuer E, Jacobs J, Du R, Wang S, Keifer OP, Cintron AF, *et al.* Amyloid-Related Imaging Abnormalities in an Aged Squirrel Monkey with Cerebral Amyloid Angiopathy. *J Alzheimers Dis* 2017;57(2):519–530. doi:10.3233/JAD-160981, PMID:28269776.
- [111] Nakamura T, Dinh TH, Asai M, Nishimaru H, Matsumoto J, Takamura Y, *et al.* Non-invasive electroencephalographical (EEG) recording system in awake monkeys. *Heliyon* 2020;6(5):e04043. doi:10.1016/j.heliyon.2020.e04043, PMID:32490247.
- [112] Chen JA, Fears SC, Jasinska AJ, Huang A, Al-Sharif NB, Scheibel KE, *et al.* Neurodegenerative disease biomarkers A $\beta$ (1-40), A $\beta$ (1-42), tau, and p-tau(181) in the vervet monkey cerebrospinal fluid: Relation to normal aging, genetic influences, and cerebral amyloid angiopathy. *Brain Behav* 2018;8(2):e00903. doi:10.1002/brb3.903, PMID:29484263.
- [113] Li ZH, He XP, Li H, He RQ, Hu XT. Age-associated changes in amyloid- $\beta$  and formaldehyde concentrations in cerebrospinal fluid of rhesus monkeys. *Zool Res* 2020;41(4):444–448. doi:10.24272/j.issn.2095-8137.2020.088, PMID:32543791.
- [114] Souder DC, Dreischmeier IA, Smith AB, Wright S, Martin SA, Sagar MAK, *et al.* Rhesus monkeys as a translational model for late-onset Alzheimer's disease. *Aging Cell* 2021;20(6):e13374. doi:10.1111/acer.13374, PMID:33951283.
- [115] Batterman KV, Cabrera PE, Moore TL, Rosene DL. T Cells Actively Infiltrate the White Matter of the Aging Monkey Brain in Relation to Increased Microglial Reactivity and Cognitive Decline. *Front Immunol* 2021;12:607691. doi:10.3389/fimmu.2021.607691, PMID:33664743.
- [116] Nagahara AH, Merrill DA, Coppola G, Tsukada S, Schroeder BE, Shaked GM, *et al.* Neuroprotective effects of brain-derived neurotrophic factor in rodent and primate models of Alzheimer's disease. *Nat Med* 2009;15(3):331–337. doi:10.1038/nm.1912, PMID:19198615.
- [117] Eberling JL, Roberts JA, Rapp PR, Tuszynski MH, Jagust WJ. Cerebral glucose metabolism and memory in aged rhesus macaques. *Neurobiol Aging* 1997;18(4):437–443. doi:10.1016/S0197-4580(97)00040-7, PMID:9330976.
- [118] Plagenhoef MR, Callahan PM, Beck WD, Blake DT, Terry AV Jr. Aged rhesus monkeys: Cognitive performance categorizations and preclinical drug testing. *Neuropharmacology* 2021;187:108489. doi:10.1016/j.neuropharm.2021.108489, PMID:33561449.
- [119] Herndon JG, Moss MB, Rosene DL, Killiany RJ. Patterns of cognitive decline in aged rhesus monkeys. *Behav Brain Res* 1997;87(1):25–34. doi:10.1016/S0166-4328(96)02256-5, PMID:9331471.
- [120] Moore TL, Killiany RJ, Herndon JG, Rosene DL, Moss MB. Impairment in abstraction and set shifting in aged rhesus monkeys. *Neurobiol Aging* 2003;24(1):125–134. doi:10.1016/S0197-4580(02)00054-4, PMID:12493558.
- [121] Moore TL, Schettler SP, Killiany RJ, Herndon JG, Luebke JJ, Moss MB, *et al.* Cognitive impairment in aged rhesus monkeys associated with monoamine receptors in the prefrontal cortex. *Behav Brain Res* 2005;160(2):208–221. doi:10.1016/j.bbr.2004.12.003, PMID:15863218.
- [122] Picq JL, Aujard F, Volk A, Dhenain M. Age-related cerebral atrophy in

- nonhuman primates predicts cognitive impairments. *Neurobiol Aging* 2012;33(6):1096–1109. doi:10.1016/j.neurobiolaging.2010.09.009, PMID:20970891.
- [123] Rahman A, Lamberty Y, Schenker E, Cella M, Languille S, Bordet R, *et al*. Effects of acute administration of donepezil or memantine on sleep-deprivation-induced spatial memory deficit in young and aged non-human primate grey mouse lemurs (*Microcebus murinus*). *PLoS One* 2017;12(9):e0184822. doi:10.1371/journal.pone.0184822, PMID:28922421.
- [124] Joly M, Ammersdörfer S, Schmidtke D, Zimmermann E. Touchscreen-based cognitive tasks reveal age-related impairment in a primate aging model, the grey mouse lemur (*Microcebus murinus*). *PLoS One* 2014;9(10):e109393. doi:10.1371/journal.pone.0109393, PMID:25299046.
- [125] Easton A, Parker K, Derrington AM, Parker A. Behaviour of marmoset monkeys in a T-maze: comparison with rats and macaque monkeys on a spatial delayed non-match to sample task. *Exp Brain Res* 2003;150(1):114–116. doi:10.1007/s00221-003-1409-5, PMID:12698223.
- [126] Lai ZC, Moss MB, Killiany RJ, Rosene DL, Herndon JG. Executive system dysfunction in the aged monkey: spatial and object reversal learning. *Neurobiol Aging* 1995;16(6):947–954. doi:10.1016/0197-4580(95)02014-4, PMID:8622786.
- [127] Lyons DM, Lopez JM, Yang C, Schatzberg AF. Stress-level cortisol treatment impairs inhibitory control of behavior in monkeys. *J Neurosci* 2000;20(20):7816–7821. doi:10.1523/JNEUROSCI.20-20-07816.2000, PMID:11027246.
- [128] Walton A, Branham A, Gash DM, Grondin R. Automated video analysis of age-related motor deficits in monkeys using EthoVision. *Neurobiol Aging* 2006;27(10):1477–1483. doi:10.1016/j.neurobiolaging.2005.08.003, PMID:16198447.
- [129] Pandya JD, Grondin R, Yonutas HM, Haghazadeh H, Gash DM, Zhang Z, *et al*. Decreased mitochondrial bioenergetics and calcium buffering capacity in the basal ganglia correlates with motor deficits in a non-human primate model of aging. *Neurobiol Aging* 2015;36(5):1903–1913. doi:10.1016/j.neurobiolaging.2015.01.018, PMID:25726361.
- [130] Shively CA, Willard SL, Register TC, Bennett AJ, Pierre PJ, Laudenslager ML, *et al*. Aging and physical mobility in group-housed Old World monkeys. *Age (Dordr)* 2012;34(5):1123–1131. doi:10.1007/s11357-011-9350-1, PMID:22203457.
- [131] Uzegbunam BC, Librizzi D, Hooshyar Yousefi B. PET Radiopharmaceuticals for Alzheimer's Disease and Parkinson's Disease Diagnosis, the Current and Future Landscape. *Molecules* 2020;25(4):977. doi:10.3390/molecules25040977, PMID:32098280.
- [132] Xu Y, Wang C, Wey HY, Liang Y, Chen Z, Choi SH, *et al*. Molecular imaging of Alzheimer's disease-related gamma-secretase in mice and nonhuman primates. *J Exp Med* 2020;217(12):e20182266. doi:10.1084/jem.20182266, PMID:32936886.
- [133] Ni R. Positron Emission Tomography in Animal Models of Alzheimer's Disease Amyloidosis: Translational Implications. *Pharmaceuticals (Basel)* 2021;14(11):1179. doi:10.3390/ph14111179, PMID:34832961.
- [134] Tsukada H, Nishiyama S, Ohba H, Kanazawa M, Kakiuchi T, Harada N. Comparing amyloid- $\beta$  deposition, neuroinflammation, glucose metabolism, and mitochondrial complex I activity in brain: a PET study in aged monkeys. *Eur J Nucl Med Mol Imaging* 2014;41(11):2127–2136. doi:10.1007/s00259-014-2821-8, PMID:24919653.
- [135] Nishiyama S, Ohba H, Kanazawa M, Kakiuchi T, Tsukada H. Comparing  $\alpha 7$  nicotinic acetylcholine receptor binding, amyloid- $\beta$  deposition, and mitochondrial complex-I function in living brain: A PET study in aged monkeys. *Synapse* 2015;69(10):475–483. doi:10.1002/syn.21842, PMID:26234533.
- [136] Nabulsi NB, Holden D, Zheng MQ, Bois F, Lin SF, Najafzadeh S, *et al*. Evaluation of (11)C-LSN3172176 as a Novel PET Tracer for Imaging M(1) Muscarinic Acetylcholine Receptors in Nonhuman Primates. *J Nucl Med* 2019;60(8):1147–1153. doi:10.2967/jnumed.118.222034, PMID:30733324.
- [137] Naganawa M, Nabulsi N, Henry S, Matuskey D, Lin SF, Sliker L, *et al*. First-in-Human Assessment of (11)C-LSN3172176, an M1 Muscarinic Acetylcholine Receptor PET Radiotracer. *J Nucl Med* 2021;62(4):553–560. doi:10.2967/jnumed.120.246967, PMID:32859711.
- [138] Ozenil M, Aronow J, Millard M, Langer T, Wadsak W, Hacker M, *et al*. Update on PET Tracer Development for Muscarinic Acetylcholine Receptors. *Pharmaceuticals (Basel)* 2021;14(6):530. doi:10.3390/ph14060530, PMID:34199622.
- [139] Damuka N, Czoty PW, Davis AT, Nader MA, Nader SH, Craft S, *et al*. PET Imaging of [(11)C]MPC-6827, a Microtubule-Based Radiotracer in Non-Human Primate Brains. *Molecules* 2020;25(10):2289. doi:10.3390/molecules25102289, PMID:32414052.
- [140] Du Y, Minn I, Foss C, Lesniak WG, Hu F, Dannals RF, *et al*. PET imaging of soluble epoxide hydrolase in non-human primate brain with [(18)F]FNDP. *EJNMMI Res* 2020;10(1):67. doi:10.1186/s13550-020-00657-7, PMID:32572592.
- [141] Lemere CA, Beierschmitt A, Iglesias M, Spooner ET, Bloom JK, Leverone JF, *et al*. Alzheimer's disease abeta vaccine reduces central nervous system abeta levels in a non-human primate, the Caribbean vervet. *Am J Pathol* 2004;165(1):283–297. doi:10.1016/S0002-9440(10)63296-8, PMID:15215183.
- [142] Trouche SG, Asuni A, Rouland S, Wisniewski T, Frangione B, Verdier JM, *et al*. Antibody response and plasma Abeta1-40 levels in young *Microcebus murinus* primates immunized with Abeta1-42 and its derivatives. *Vaccine* 2009;27(7):957–964. doi:10.1016/j.vaccine.2008.12.012S0264-410X(08)01724-6, PMID:19114076.
- [143] Yano A, Ito K, Miwa Y, Kanazawa Y, Chiba A, Iigo Y, *et al*. The Peptide Vaccine Combined with Prior Immunization of a Conventional Diphtheria-Tetanus Toxoid Vaccine Induced Amyloid  $\beta$  Binding Antibodies on *Cynomolgus* Monkeys and Guinea Pigs. *J Immunol Res* 2015;2015:786501. doi:10.1155/2015/786501, PMID:26539559.
- [144] Vukicevic M, Fiorini E, Siegert S, Carpintero R, Rincon-Restrepo M, Lopez-Deber P, *et al*. An amyloid beta vaccine that safely drives immunity to a key pathological species in Alzheimer's disease: pyroglutamate amyloid beta. *Brain Commun* 2022;4(1):fcac022. doi:10.1093/braincomms/fcac022, PMID:35479516.
- [145] Kofler J, Lopresti B, Janssen C, Trichel AM, Masliah E, Finn OJ, *et al*. Preventive immunization of aged and juvenile non-human primates to  $\beta$ -amyloid. *J Neuroinflammation* 2012;9:84. doi:10.1186/1742-2094-9-84, PMID:22554253.
- [146] Vaz M, Silvestre S. Alzheimer's disease: Recent treatment strategies. *Eur J Pharmacol* 2020;887:173554. doi:10.1016/j.ejphar.2020.173554, PMID:32941929.
- [147] Zheng H, Niu S, Zhao H, Li S, Jiao J. Donepezil improves the cognitive impairment in a tree shrew model of Alzheimer's disease induced by amyloid- $\beta$ (1-40) via activating the BDNF/TrkB signal pathway. *Metab Brain Dis* 2018;33(6):1961–1974. doi:10.1007/s11011-018-0303-6, PMID:30105614.
- [148] Li Y, Laws SM, Miles LA, Wiley JS, Huang X, Masters CL, *et al*. Genomics of Alzheimer's disease implicates the innate and adaptive immune systems. *Cell Mol Life Sci* 2021;78(23):7397–7426. doi:10.1007/s00018-021-03986-5, PMID:34708251.
- [149] Boado RJ, Lu JZ, Hui EK, Pardridge WM. IgG-single chain Fv fusion protein therapeutic for Alzheimer's disease: Expression in CHO cells and pharmacokinetics and brain delivery in the rhesus monkey. *Biotechnol Bioeng* 2010;105(3):627–635. doi:10.1002/bit.22576, PMID:19816967.
- [150] Gao L, Zhang Y, Sterling K, Song W. Brain-derived neurotrophic factor in Alzheimer's disease and its pharmaceutical potential. *Transl Neurodegener* 2022;11(1):4. doi:10.1186/s40035-022-00279-0, PMID:35090576.
- [151] Lange HS, Vardigan JD, Cannon CE, Puri V, Henze DA, Uslander JM. Effects of a novel M4 muscarinic positive allosteric modulator on behavior and cognitive deficits relevant to Alzheimer's disease and schizophrenia in rhesus monkey. *Neuropharmacology* 2021;197:108754. doi:10.1016/j.neuropharm.2021.108754, PMID:34389398.
- [152] Pushpakom S, Iorio F, Eyers PA, Escott KJ, Hopper S, Wells A, *et al*. Drug repurposing: progress, challenges and recommendations. *Nat Rev Drug Discov* 2019;18(1):41–58. doi:10.1038/nrd.2018.168, PMID:30310233.
- [153] Lee HJ, Seo HI, Cha HY, Yang YJ, Kwon SH, Yang SJ. Diabetes and Alzheimer's Disease: Mechanisms and Nutritional Aspects. *Clin Nutr Res* 2018;7(4):229–240. doi:10.7762/cnr.2018.7.4.229, PMID:30406052.
- [154] Batista AF, Forny-Germano L, Clarke JR, Lyra E Silva NM, Brito-Moreira J, Boehnke SE, *et al*. The diabetes drug liraglutide reverses cognitive impairment in mice and attenuates insulin receptor and

- synaptic pathology in a non-human primate model of Alzheimer's disease. *J Pathol* 2018;245(1):85–100. doi:10.1002/path.5056, PMID: 29435980.
- [155] Blackburn JK, Jamwal S, Wang W, Elsworth JD. Pioglitazone transiently stimulates paraoxonase-2 expression in male nonhuman primate brain: Implications for sex-specific therapeutics in neurodegenerative disorders. *Neurochem Int* 2022;152:105222. doi:10.1016/j.neuint.2021.105222, PMID:34767873.
- [156] Li Y, Huang X, Fowler C, Lim YY, Laws SM, Faux N, *et al*. Identification of Leukocyte Surface P2X7 as a Biomarker Associated with Alzheimer's Disease. *Int J Mol Sci* 2022;23(14):7867. doi:10.3390/ijms23147867, PMID:35887215.
- [157] Huang X, Li Y, Fowler C, Doecke JD, Lim YY, Drysdale C, *et al*. Leukocyte surface biomarkers implicate deficits of innate immunity in sporadic Alzheimer's disease. *Alzheimers Dement* 2022. doi:10.1002/alz.12813, PMID:36349985.
- [158] Sachdeva D, Burns A. Dimebolin in dementia. *CNS Neurosci Ther* 2011;17(3):199–205. doi:10.1111/j.1755-5949.2010.00156.x, PMID: 20553307.
- [159] Webster SJ, Wilson CA, Lee CH, Mohler EG, Terry AV Jr, Buccafusco JJ. The acute effects of dimebolin, a potential Alzheimer's disease treatment, on working memory in rhesus monkeys. *Br J Pharmacol* 2011;164(3):970–978. doi:10.1111/j.1476-5381.2011.01432.x, PMID:21486290.
- [160] Ling IF, Golde TE, Galasko DR, Koo EH. Modulation of A $\beta$ 42 in vivo by  $\gamma$ -secretase modulator in primates and humans. *Alzheimers Res Ther* 2015;7(1):55. doi:10.1186/s13195-015-0137-y137, PMID:26244059.
- [161] Dokmeci D. Ibuprofen and Alzheimer's disease. *Folia Med (Plovdiv)* 2004;46(2):5–10. PMID:15506544.
- [162] Bhatti GK, Reddy AP, Reddy PH, Bhatti JS. Lifestyle Modifications and Nutritional Interventions in Aging-Associated Cognitive Decline and Alzheimer's Disease. *Front Aging Neurosci* 2019;11:369. doi:10.3389/fnagi.2019.00369, PMID:31998117.
- [163] Qin W, Chachich M, Lane M, Roth G, Bryant M, de Cabo R, *et al*. Calorie restriction attenuates Alzheimer's disease type brain amyloidosis in Squirrel monkeys (*Saimiri sciureus*). *J Alzheimers Dis* 2006;10(4):417–422. doi:10.3233/jad-2006-10411, PMID:17183154.
- [164] Willette AA, Coe CL, Colman RJ, Bendlin BB, Kastman EK, Field AS, *et al*. Calorie restriction reduces psychological stress reactivity and its association with brain volume and microstructure in aged rhesus monkeys. *Psychoneuroendocrinology* 2012;37(7):903–916. doi:10.1016/j.psyneuen.2011.10.006, PMID:22119476.
- [165] Cox PA, Davis DA, Mash DC, Metcalf JS, Banack SA. Dietary exposure to an environmental toxin triggers neurofibrillary tangles and amyloid deposits in the brain. *Proc Biol Sci* 2016;283:1823. doi:10.1098/rspb.2015.2397, PMID:26791617.
- [166] Cox PA, Metcalf JS. Traditional Food Items in Ogimi, Okinawa: L-Serine Content and the Potential for Neuroprotection. *Curr Nutr Rep* 2017;6(1):24–31. doi:10.1007/s13668-017-0191-0, PMID:28331770.
- [167] Frye BM, Craft S, Register TC, Andrews RN, Appt SE, Vitolins MZ, *et al*. Diet, psychosocial stress, and Alzheimer's disease-related neuroanatomy in female nonhuman primates. *Alzheimers Dement* 2021;17(5):733–744. doi:10.1002/alz.12232, PMID:33270373.
- [168] Li J, Huang Q, Chen J, Qi H, Liu J, Chen Z, *et al*. Neuroprotective Potentials of Panax Ginseng Against Alzheimer's Disease: A Review of Preclinical and Clinical Evidences. *Front Pharmacol* 2021;12:688490. doi:10.3389/fphar.2021.688490, PMID:34149431.
- [169] Wang L, Lu J, Zeng Y, Guo Y, Wu C, Zhao H, *et al*. Improving Alzheimer's disease by altering gut microbiota in tree shrews with ginsenoside Rg1. *FEMS Microbiol Lett* 2020;367(4):fnaa011. doi:10.1093/femsle/fnaa011, PMID:31950993.
- [170] Guo Y, Wang L, Lu J, Jiao J, Yang Y, Zhao H, *et al*. Ginsenoside Rg1 improves cognitive capability and affects the microbiota of large intestine of tree shrew model for Alzheimer's disease. *Mol Med Rep* 2021;23(4):291. doi:10.3892/mmr.2021.11931, PMID:33649817.
- [171] Yang Y, Wang L, Zhang C, Guo Y, Li J, Wu C, *et al*. Ginsenoside Rg1 improves Alzheimer's disease by regulating oxidative stress, apoptosis, and neuroinflammation through Wnt/GSK-3 $\beta$ / $\beta$ -catenin signaling pathway. *Chem Biol Drug Des* 2022;99(6):884–896. doi:10.1111/cbdd.14041, PMID:35313087.